

RESEARCH ARTICLE



The ion channel TRPM8 is a direct target of the immunosuppressant rapamycin in primary sensory neurons

José Miguel Arcas | Khalid Oudaha | Alejandro González |
 Jorge Fernández-Trillo | Francisco Andrés Peralta | Júlia Castro-Marsal |
 Seyma Poyraz | Francisco Taberner | Salvador Sala | Elvira de la Peña |
 Ana Gomis | Félix Viana

Instituto de Neurociencias, Universidad Miguel Hernández-CSIC, San Juan de Alicante, Spain

Correspondence

Félix Viana, Instituto de Neurociencias, Universidad Miguel Hernández-CSIC, San Juan de Alicante 03550, Spain.
 Email: felix.viana@umh.es

Present address

Alejandro González, Karolinska Institutet, Stockholm, Sweden.

Funding information

Generalitat Valenciana, Grant/Award Numbers: GRISOLIA/2019/089, PROMETEO/2021/03; Ministerio de Ciencia e Innovación, Grant/Award Numbers: CEX2021-001165-S, PID2019-108194RB-I00/AEI/10.13039/501100011033; Consejo Superior de Investigaciones Científicas, Grant/Award Number: JAEINT_22_01043; Fundacion ICAR, Grant/Award Number: ionRAPA Grant; European Regional Development Fund

Background and Purpose: The mechanistic target of rapamycin (mTOR) signalling pathway is a key regulator of cell growth and metabolism. Its deregulation is implicated in several diseases. The macrolide rapamycin, a specific inhibitor of mTOR, has immunosuppressive, anti-inflammatory and antiproliferative properties. Recently, we identified tacrolimus, another macrolide immunosuppressant, as a novel activator of TRPM8 ion channels, involved in cold temperature sensing, thermoregulation, tearing and cold pain. We hypothesized that rapamycin may also have agonist activity on TRPM8 channels.

Experimental Approach: Using calcium imaging and electrophysiology in transfected HEK293 cells and wildtype or *Trpm8* KO mouse DRG neurons, we characterized rapamycin's effects on TRPM8 channels. We also examined the effects of rapamycin on tearing in mice.

Key Results: Micromolar concentrations of rapamycin activated rat and mouse TRPM8 channels directly and potentiated cold-evoked responses, effects also observed in human TRPM8 channels. In cultured mouse DRG neurons, rapamycin increased intracellular calcium levels almost exclusively in cold-sensitive neurons. Responses were markedly decreased in *Trpm8* KO mice or by TRPM8 channel antagonists. Cutaneous cold thermoreceptor endings were also activated by rapamycin. Topical application of rapamycin to the eye surface evokes tearing in mice by a TRPM8-dependent mechanism.

Conclusion and Implications: These results identify TRPM8 cationic channels in sensory neurons as novel molecular targets of the immunosuppressant rapamycin. These findings may help explain some of its therapeutic effects after topical application to the skin and the eye surface. Moreover, rapamycin could be used as an experimental tool in the clinic to explore cold thermoreceptors.

Abbreviations: ABS, acrylonitrile butadiene styrene; AM, acetoxymethyl ester; DED, dry eye disease; DMSO, dimethyl sulfoxide; DRG, dorsal root ganglion; EGFP, enhanced green fluorescent protein; EDTA, ethylene diamine tetra-acetic acid; EGTA, ethylene glycol tetra-acetic acid; EYFP, enhanced yellow fluorescent protein; FDA, Food and Drug Administration; HBSS, Hank's balanced salt solution; KO, knockout; mTOR, mechanistic target of rapamycin; PCR, polymerase chain reaction; PIP2, phosphatidylinositol 4,5-bisphosphate; SD, standard deviation; SEM, standard error of mean.

This is an open access article under the terms of the [Creative Commons Attribution-NonCommercial-NoDerivs](https://creativecommons.org/licenses/by-nc-nd/4.0/) License, which permits use and distribution in any medium, provided the original work is properly cited, the use is non-commercial and no modifications or adaptations are made.

© 2024 The Authors. *British Journal of Pharmacology* published by John Wiley & Sons Ltd on behalf of British Pharmacological Society.

KEYWORDS

ageing, cold, dry eye disease, mTOR, pain, thermoregulation

1 | INTRODUCTION

Rapamycin is a natural macrolide compound, isolated in 1975 from the bacterium *Streptomyces hygroscopicus* in soil samples from Rapa Nui, also known as Easter Island (Vezina et al., 1975). It was originally identified as an antifungal agent and later shown to have immunosuppressive properties (see Benjamin et al., 2011). Rapamycin (sirolimus) and its analogues, called rapalogs, have important clinical applications, including their use as immunosuppressants to prevent organ rejection and as tumour suppressors. **Everolimus** (RAD001), a derivative of rapamycin with improved water solubility, is an FDA approved drug for the treatment of various solid tumours, including neuroendocrine tumours, breast cancer, renal cell carcinoma and sub-ependymal giant cell astrocytoma (see Li et al., 2014; Seto, 2012). Topical application of rapamycin is beneficial in ocular inflammatory disorders, including dry eye disease (Spatola et al., 2018). In addition, rapamycin has been used extensively as a research tool (see Kunz & Hall, 1993).

Rapamycin acts by inhibiting the mechanistic target of rapamycin (**mTOR**) (Heitman et al., 1991; Johnson et al., 2013), a key kinase for cellular growth and proliferation, sensing and integrating multiple metabolic signals: growth factors, nutrients, metabolites and oxygen levels (Kennedy & Lamming, 2016). Rapamycin and derivatives bind to its receptor, **FKBP12**, which directly interacts with the mTORC1 complex, inhibiting its downstream signalling. The inhibition of mTORC1 disrupts glycolytic pathways, decreases lipolysis and induces autophagy, inhibiting cell proliferation (Saxton & Sabatini, 2017). Pharmacological inhibition of mTORC1 is also being explored as neuroprotectant in various neurodegenerative diseases.

Rapamycin administration has multiple effects on organism biology, which are still poorly understood and require further study. The recent discovery that rapamycin can extend the lifespan in numerous species, from yeast to mice, and improve age-related functional decline in those species, has generated great excitement in the field of ageing biology (Bitto et al., 2016; Harrison et al., 2009; Wilkinson et al., 2012). Indeed, this is one of the few examples of a clinically approved drug capable of slowing the ageing process in mammals.

Recently, we identified **tacrolimus** (FK-506), a different macrolide immunosuppressant targeting calcineurin, as an agonist of **TRPM8** channels (Arcas et al., 2019), a cold- and menthol-activated cationic channel (McKemy et al., 2002; Peier et al., 2002) expressed in the soma of a subset of small diameter primary sensory neurons and their peripheral terminals (Dhaka et al., 2008; Takashima et al., 2007). In mammals, TRPM8 channels play a major role in cold temperature detection, thermoregulation and cold pain (see Almaraz et al., 2014). Moreover, agonists of TRPM8 channels promote ocular tearing and blinking (Parra et al., 2010; Quallo et al., 2015) and can ameliorate the symptoms of dry eye disease. In addition, *TRPM8* is overexpressed in

What is already known

- TRPM8 is a polymodal channel involved in cold detection, thermoregulation, tearing and cold pain.
- Tacrolimus, a macrolide immunosuppressor, is an agonist of cold-activated TRPM8 channels.

What does this study add

- The macrolide rapamycin also activates directly TRPM8 channels in mouse sensory neurons and human TRPM8.
- Rapamycin stimulates tearing in mice in a TRPM8-dependent manner.

What is the clinical significance

- Rapamycin, an FDA-approved drug, shows agonist activity on TRPM8 channels.
- Beneficial effects of rapamycin and other macrolides on inflammatory ocular disorders may involve TRPM8 activation.

prostate cancers and other solid tumours, making it an interesting target and prognostic marker for the disease (Bidaux et al., 2016; Zhang & Barritt, 2006).

Here, we asked whether rapamycin and its analogue, everolimus, share agonist activity on TRPM8 channels. We found that both compounds activate recombinant TRPM8 channels from various species, including humans, and mouse TRPM8-expressing sensory neurons, generalizing macrolide immunosuppressants as a novel, clinically relevant class of mammalian TRPM8 channel modulators.

2 | METHODS

2.1 | Animals

All animal care and experimental procedures complied with the Spanish Royal Decree 53/2013 and the European Community Council directive 2016/63/EU, regulating the use of animals in research. Animal studies are reported in compliance with the ARRIVE guidelines (Percie du Sert et al., 2020) and with the recommendations made by the *British Journal of Pharmacology* (Lilley et al., 2020).

Studies were performed on young adult (1 to 4 months old) mice of either sex. Mice were bred at the Universidad Miguel Hernández Animal Research Facilities (ES-119-002001) and kept in a barrier facility under 12/12 h light/ dark cycle with food and water ad libitum. Wild type (WT) mice were of the C57Bl/6J strain.

Two transgenic mouse lines were used for calcium imaging experiments and electrophysiological recordings on DRG cultures. In *Trpm8*^{BAC-EYFP} mice, the fluorescent protein EYFP is expressed under the *Trpm8* promoter (Morenilla-Palao et al., 2014). For experiments with *Trpm8* KO mice, we used a transgenic knockin line, *Trpm8*^{EGFPf} (*IMSR_JAX:014581*), in which the *Trpm8* locus was disrupted and far-nesylated EGFP was inserted in frame with the *Trpm8* start codon (Dhaka et al., 2007). Homozygous mice (*Trpm8*^{EGFPf/EGFPf}) are null for TRPM8 (Dhaka et al., 2007; Parra et al., 2010). As previously described, to enhance EGFPf expression the lox-P-flanked neomycin selection cassette introduced into the *Trpm8* locus during the generation of the transgene was excised (Dhaka et al., 2008). Both transgenic lines allowed the identification of TRPM8-expressing cells by the expression of EYFP or EGFP fluorescence. Moreover, *Trpm8*^{EGFPf/+} (i.e., heterozygous) allowed recordings from EGFP(+) neurons with one functional copy of TRPM8. The genotype of transgenic mice was established by PCR.

Experiments in cultured DRG neurons and behavioural experiments were performed on animals of either sex. Experiments on the firing of mouse afferents (i.e., skin-nerve preparation) were performed on male mice only due to limited availability of female mice at the time. TRPM8 channels are expressed in both sexes and the effect of rapamycin on TRPM8 channels is direct. We did not observe any differences in the results between male and female animals, so the data were pooled.

2.2 | Culture and transfection of mammalian cell lines

HEK293 cells (ECACC Cat# 85120602, [RRID:CVCL_0045](#)) were maintained in DMEM plus Glutamax, supplemented with 10% fetal bovine serum, 100 U·ml⁻¹ penicillin (Gibco) and 100 µg·ml⁻¹ streptomycin (Gibco), incubated at 37°C in a 5% CO₂ atmosphere. HEK293 cells were plated in 24-well dishes at 2 × 10⁵ cells per well and transiently transfected with Lipofectamine 2000 (Thermo Fisher Scientific). When necessary, we co-transfected the cells with 1 µg of TRPM8 channel plasmid (from different species) and 0.5 µg of EGFP or mCherry plasmid (Addgene_84329) (van Unen et al., 2016). Enhanced Green fluorescent protein (EGFP) was expressed from the pGREEN LANTERN™-1 vector (Life Technologies). For the transfection, 2 µl of Lipofectamine 2000 was mixed with the DNA in 100 µl of OptiMem (Thermo Fisher Scientific), a reduced serum media. Electrophysiological and calcium imaging recordings took place 24–36 h after transfection. The evening before the experiment, cells were trypsinized (0.25% trypsin-EGTA) and reseeded at lower density in 12-mm diameter glass coverslips previously treated with poly-L lysine (0.01%, Sigma-Aldrich).

The expression vectors used and their source were as follows: mouse TRPM8 (NM_134252) in pcDNA5, kindly provided by Ardem

Patapoutian (Scripps Research Institute, La Jolla, USA), was used as a wildtype TRPM8. Human TRPM8 in pcDNA3 (Veit Flockerzi, Saarland University), human **TRPA1** in pCMV6-AC-GFP (Veit Flockerzi, Saarland University), rat **TRPV1** in pcDNA3 (David Julius, UCSF) and human TRPV1 in pcDNA3(+) (Andreas Leffler, Hannover Medical School) were also transiently transfected in HEK293 cells using the same techniques. The menthol-insensitive mouse TRPM8-Y745H mutant was generated by site-directed mutagenesis (Malkia et al., 2009).

HEK293 cells stably expressing rat TRPM8 channels (CR#1 cells) (Brauchi et al., 2004) were cultured in DMEM containing 10% of fetal bovine serum, 100 U·ml⁻¹ penicillin, 100 mg·ml⁻¹ streptomycin (Gibco) and 450 µg·ml⁻¹ geneticin (G418).

2.3 | DRG cultures

Adult mice of either sex (1–4 months) were anaesthetised with isoflurane and decapitated. The spinal cord was isolated, and dorsal root ganglia (DRG) were dissected out from all spinal segments and maintained in ice-cold HBSS solution. After isolation, DRGs were incubated with collagenase type XI (Sigma) and dispase II for 30–45 min in Ca²⁺- and Mg²⁺-free HBSS medium at 37°C in 5% CO₂. Thereafter, DRG ganglia were mechanically dissociated by passing 15–20 times through a 1-ml pipette tip and filtered through a 70 µm nylon filter. Neurons were harvested by centrifugation at 172 g (room temperature) during 5 min. The resultant pellet was resuspended in Minimum Essential Medium (MEM) supplemented with 10% FBS, 1% MEM-vit, 100 U·ml⁻¹ penicillin (Gibco), 100 mg·ml⁻¹ streptomycin (Gibco) and plated on poly-L-lysine-coated glass coverslips. Electrophysiological and calcium-imaging recordings were performed after 12–36 h in culture.

2.4 | Fluorescence Ca²⁺ imaging

Ratiometric calcium imaging experiments were conducted with the fluorescent indicator Fura-2 (Thermo Fisher Scientific). DRG neurons or HEK293 cells were incubated with 5 µM Fura-2 AM and 0.2% Pluronic (Thermo Fisher Scientific) (prepared from a 200 mg·ml⁻¹ stock solution in DMSO) for 45 min at 37°C in standard extracellular solution. Fluorescence measurements were obtained on a Leica inverted microscope fitted with an Imago-QE Sencam camera (PCO). Fura-2 was excited at 340 and 380 nm (excitation time 60 ms) with a rapid switching monochromator (TILL Photonics) or an LED-based system (Lambda OBC, Sutter Instruments). Mean fluorescence intensity ratios (F340/F380) were displayed online with TillVision (TILL Photonics) or Metafluor (Molecular Devices, San Jose, CA, USA) software. The standard bath solution (290 mOsm·kg⁻¹) contained (in mM): 140 NaCl, 3 KCl, 2.4 CaCl₂, 1.3 MgCl₂, 10 HEPES, and 10 glucose, adjusted to a pH of 7.4 with NaOH. Calcium imaging recordings were performed at a basal temperature of 33 ± 1°C. Before the start of the experiment, an image of the microscopic field was obtained with transmitted light and under 460 nm excitation wavelength, in order to identify fluorescent cells.

Responses to agonists were calculated by measuring the peak ratio values, after subtracting the mean baseline fluorescence ratio during the 15 seconds previous to agonist application. Responses were scored as positive if the increase in fluorescence (Δ Fura2 ratio) was >0.08 .

2.5 | Electrophysiology in cultured cells

Whole-cell voltage- and current-clamp recordings were obtained from mouse DRG neurons or transiently transfected HEK293 cells with borosilicate glass patch-pipettes (Sutter Instruments, 4–8 M Ω resistance) and were performed simultaneously with temperature recordings. Signals were recorded with an Axopatch 200B patch-clamp amplifier (Molecular Devices) and digitized through a Digidata 1322A (Molecular Devices). Stimulus delivery and data acquisition were performed using pCLAMP9 software (Molecular Devices).

For neuronal recordings, we used the standard bath solution (see above) at a basal temperature of 33°C. The intracellular solution (280 mOsm·kg⁻¹) contained (in mM): 115 K-gluconate, 25 KCl, 9 NaCl, 10 HEPES, 0.2 EGTA, 1 MgCl₂, 1 Na₂GTP and 3 K₂ATP, adjusted to pH 7.35 with KOH. In voltage-clamp recordings amplifier gain was set at x1, sampling rate was set to 10 kHz and the signal was filtered at 2 kHz. Neurons were voltage-clamped at a potential of -60 mV. For current clamp recordings gain was set at x10, acquisition rate was 50 kHz and the signal was filtered at 10 kHz. Once in the whole-cell configuration, resting membrane potential was measured. In neurons that fired action potentials at rest, a small DC current was injected to bring the cell to around -55 mV.

For electrophysiological experiments in HEK293 cells, to minimize desensitization of TRPM8 channel responses, a calcium-free extracellular solution was used (in mM): 144.8 NaCl, 3 KCl, 1 EGTA, 1.3 MgCl₂, 10 HEPES, and 10 glucose (290 mOsm·kg⁻¹, pH adjusted to 7.4 with NaOH). The intracellular solution for HEK293 recordings was (in mM): 135 CsCl, 2 MgCl₂, 10 HEPES, 1 EGTA, 5 Na₂ATP and 0.1 NaGTP, adjusted to pH 7.4 with CsOH (280 mOsm·kg⁻¹). For experiments examining the dose-dependence of rapamycin, the extracellular solutions contained (in mM): 150 NaCl, 10 EDTA, 10 HEPES, 10 glucose (332 mOsm·kg⁻¹, pH adjusted to 7.4 with NaOH). In these experiments, the intracellular solution was (in mM): 150 NaCl, 3 MgCl₂, 10 HEPES, 5 EGTA (300 mOsm·kg⁻¹, pH adjusted to 7.2 with NaOH). Due to the pH adjustment of the EDTA stock solution with NaOH, we calculated an excess of 19 mM Na in the extracellular solution, relative to the intracellular Na concentration. Recordings were performed at a basal temperature of 33 ± 1°C.

After a Gigaohm seal was formed and the whole-cell configuration was established, cells were voltage-clamped at a potential of -60 mV. To estimate shifts in the voltage dependence of TRPM8 activation during cold and agonist application, current-voltage (I-V) relationships obtained from repetitive (0.33 Hz) voltage ramps (-100 to +150 mV, 400 ms duration) were fitted with Origin BotzIV function (OriginPro version 2021. OriginLab Corporation, Northampton, MA, USA) a function that combines a linear conductance multiplied by a Boltzmann activation term:

$$I = G \times (V - E_{rev}) / (1 + \exp((V_{1/2} - V)/dx))$$

where G is the whole-cell conductance, E_{rev} is the reversal potential of the current, $V_{1/2}$ is the potential for half-maximal activation and dx is the slope factor.

We determined the E_{rev} parameter independently for each condition by measuring the average voltage at which the current reversed sign, which was then kept constant during the fitting process. While the G value was shared between all conditions, $V_{1/2}$ and dx were left free to vary for each condition. The ramps were analysed with WinASCD software package (Prof. G. Droogmans, Laboratory of Physiology, KU Leuven).

2.6 | Single channel recordings

Gating of TRPM8 channels by agonists requires the intracellular presence of PIP₂ and polyphosphates (Zakharian et al., 2009). To minimize fluctuations in the concentration of these intracellular mediators, we characterized channel activity during cell-attached recordings.

Single channel recordings were obtained at room temperature (25 ± 0.5°C), from HEK2923 cells transiently transfected with mTRPM8 and mCherry using a HEKA EPC10 amplifier with PatchMaster software (HEKA Elektronik, Lambrecht, Germany). Borosilicate glass patch pipettes were fire-polished to a resistance of 7–10 M Ω . Current signal was sampled at 50 kHz and filtered at 3 kHz.

After obtaining a Gigaohm seal, the standard bath solution (in mM): 140 NaCl, 3 KCl, 2.4 CaCl₂, 1.3 MgCl₂, 10 glucose, 10 HEPES, pH: 7.4, was switched to a calcium-free solution containing 145 NaCl, 3 KCl, 10 glucose, 10 HEPES, 1 EGTA, pH: 7.4, to minimize TRPM8 channel desensitization. The pipette solution contained (in mM): 140 KCl, 0.6 MgCl₂, 10 HEPES, 1 EGTA, pH: 7.4. All-point histograms of the channel current were fitted to a double Gaussian function (dashed line in red). The single-channel current was calculated from the difference in the two fitted peak values. Single-channel conductance events, all points' histograms, open probability, and other parameters were identified and analysed using Nest-o-Patch 2.1.9.8 (<https://sourceforge.net/p/nestopatch/wiki/Home/>) and Clampfit 9.2 (Molecular Devices).

2.7 | Temperature stimulation

Glass coverslip pieces with cultured cells were placed in a microchamber and continuously perfused with solutions warmed at 33 ± 1°C. The temperature was adjusted with a Peltier device (CoolSolutions, Cork, Ireland) placed at the inlet of the chamber, and controlled by a feedback device (Reid et al., 2001). Cold sensitivity was investigated with a temperature drop to approximately 18°C. The bath temperature was monitored with an IT-18 T-thermocouple connected to a Physitemp BAT-12 micro- probe thermometer (Physitemp Instruments) and digitized with an Axon Digidata 1322A AD converter running Clampex 9 software (Molecular Devices).

2.8 | Isolated skin-nerve preparation

Extracellular recordings from single cutaneous primary afferent axons in an isolated mouse skin–saphenous nerve preparation were obtained following previously published procedures (Roza et al., 2006; Zimmermann et al., 2009). In brief, adult male C57Bl/6J mice were killed by cervical dislocation and the hairy skin from either hind paw, with the saphenous nerve attached, was dissected free from underlying muscles and placed in a custom made Teflon recording chamber with the corium side up (Zimmermann et al., 2009).

The chamber containing the preparation was continuously superfused at a rate of 4 ml·min⁻¹ with oxygenated external solution consisting of (in mM): 107.8 NaCl, 26.2 NaHCO₃, 9.64 sodium gluconate, 7.6 sucrose, 5.55 glucose, 3.5 KCl, 1.67 NaH₂PO₄, 1.53 CaCl₂ and 0.69 MgSO₄, which was adjusted to pH 7.4 by continuously gassing with 95% oxygen–5% CO₂. Temperature of the solution was maintained around 34°C with a SC-20 in-line heater/cooler system, driven by a CL-100 bipolar temperature controller (Warner Instruments).

After pulling back the perineurium with Dumont #5SF forceps, a small bundle of fibres was aspirated into a patch-pipette connected to a high gain AC differential amplifier (model DAM 80; World Precision Instruments). A reference electrode was positioned inside the chamber. Input signals were amplified, digitized (CED Micro1401–3; Cambridge Electronic Design) at 25 kHz and stored in the hard drive of a PC for off-line analysis. For recording and off-line analysis, the Spike 2 software package was used (Cambridge Electronic Design).

A small, cone-shaped piece of frozen external solution was moved slowly over the corium side of the skin and used to identify cold spots: brisk thermoreceptor fibre activity was evoked by the ice cone when in the immediate vicinity of the receptive field, and this activity stopped shortly after removing the stimulus. Cold spots, identified in this way, were then isolated from the surrounding tissue with a small ABS thermoplastic ring, and delivery of the subsequent cold and chemical stimuli were restricted to a circular area (5 mm diameter) of the skin. Cold stimuli were performed with solutions flowing through a Peltier system custom-designed to deliver a small volume of solution inside the ring isolating the skin area. Starting from a baseline temperature of 34–35°C, the temperature reached ~ 12°C in about 50 seconds.

In control conditions, at the baseline temperature of 34–35°C, cold thermoreceptors were silent, firing action potentials during the cooling ramp. The cold threshold was defined as the temperature corresponding to the first spike during a cooling ramp. When chemical sensitization led to the appearance of ongoing activity already at basal temperature, cold threshold was taken as the mean temperature during the 60 s preceding the start of the cooling ramp. Chemical sensitivity of single fibres was tested with consecutive applications of rapamycin (30 µM), followed by menthol (50 µM) after a period of wash. Chemical sensitivity during recordings at 34°C was defined as the presence of at least 20 spikes during a period of 2 min before the cooling ramp. In order to explore their effects on cold sensitivity, a cold temperature ramp was also applied in the presence of rapamycin or menthol.

2.9 | Mathematical modelling of cold thermoreceptor activity

To simulate the effect of temperature changes and agonist applications on cold thermoreceptor activity, we used the model of cold-sensitive neurons with TRPM8 channels originally described by Patricio Orio and colleagues for cold sensitive nerve endings (Olivares et al., 2015) and later for trigeminal neurons (Rivera et al., 2021). The equations and parameters are as described in Rivera et al., except for the reversal potential of the depolarizing currents that was set to +70 mV, and that no white noise current was used in order to get more reproducible results. All 52 parameter sets described by Rivera et al. were used to simulate neurons with different temperature thresholds. The model was implemented in NEURON and controlled with Python 3.8 (Carnevale & Hines, 2006; Hines et al., 2009).

To emulate our experimental protocol, a double temperature ramp was applied with 120 s interval between the two; each ramp consisted in cooling from 34 to 18°C in 12 s and then warming back to 34°C in 14 s. The first ramp starts at $t = 30$ s.

We simulated the application of a pulse of TRPM8 agonist by changing g_{M8} , V_{half} or both. The agonist pulse was applied at $t = 120$ s and maintained for 90 s approximately. Thus, the second temperature ramp is applied while the agonist pulse is on. The total simulation time is 225 s.

In *Current-Clamp* simulations, a temperature threshold is defined as the temperature at which the first action potential is fired. The time at which an action potential is fired is given by the time it crosses the 0 mV from below, and the instantaneous firing frequency is defined as the inverse of the time between two consecutive action potentials. Thus, two temperature thresholds are measured, one for each ramp (i.e., the first in control conditions and the second in the presence of agonist). Also, two corresponding values for the maximum, and average firing frequency are measured, for the first and second temperature ramps and at the beginning of the agonist pulse.

In *Voltage-Clamp* simulations, the membrane potential is clamped at –60 mV and the I_{M8} current is recorded using the same temperature ramp and agonist pulse as described above. The peak I_{M8} current is measured when elicited by a cold ramp, an agonist pulse, or both.

We analysed the results of the simulations with R (R Core Team, 2022), and the Python packages NumPy (Harris et al., 2020), SciPy (Virtanen et al., 2020) and Matplotlib (v3.84) (Hunter, 2007).

2.10 | Behavioural assessment of tearing

Adult male and female mice, C57BL/6J ($n = 15$) or *Trpm8* KO ($n = 15$) (Dhaka et al., 2008), were anaesthetized by intraperitoneal injection of a mixture of ketamine hydrochloride (80 mg·kg⁻¹, Imalgene 1000; Laboratorios Merial S.A., Barcelona, Spain) and xylazine hydrochloride (5 mg·kg⁻¹, Rompun; Bayer Hispania S.L., Barcelona, Spain). Tear flow was measured in both eyes, using phenol red threads (Zone-Quick, Menicon Pharma S.A., Illkirch Graffenstaden, France), after applications of a drop (2 µl) of 1% rapamycin in one eye or vehicle (8% ethanol, 2% Cremophor in saline) in the other using a graduated micropipette (Gilson Pipetman P2). Each solution was applied for

2 min. Thereafter, excess fluid was removed using a sterile absorbent swab (Sugi® Eyespear pointed tip, Kettencach GmbH & Co., Germany). After a rest period of 5 min, a phenol red thread was gently placed between the lower lid and the bulbar conjunctiva at the nasal angle during 1 min. To quantify the staining of the threads, the wetted length was measured under a stereomicroscope. The eye receiving rapamycin was randomly chosen for each mouse. The experimenters were blind to the animal's genetic background and treatment. After measurements, animals were humanely killed according to the approved protocol.

2.11 | Data and statistical analysis

The data and statistical analysis in this study complied with the recommendations and requirements on experimental design and analysis of the BJP (Curtis et al., 2022). For most in vitro protocols, blinding was not feasible as experiments were conducted by an individual experimenter. During in vivo experiments, the experimenter was blind to animal phenotype and treatment. All experimental groups had a size of 5 or larger. Coverslips with plated cells or neurons were only used once (i.e., a single imaging field or a single neuron). Data were obtained from multiple experiments or animals, as described in figure legends, generally on different dates.

To estimate shifts in the voltage dependence of TRPM8 channel activation, current–voltage (I–V) relationships obtained from repetitive (0.33 Hz) voltage ramps (–100 to +150 mV, 400-ms duration) were fitted with a function that combines a linear conductance multiplied by a Boltzmann activation term:

$$I = G \times (V - E_{\text{rev}}) / (1 + \exp((V_{1/2} - V) / dx))$$

where G is the whole-cell conductance, E_{rev} is the reversal potential of the current, $V_{1/2}$ is the potential for half-maximal activation and dx is the slope factor. The G value obtained for a high menthol concentration (800 μM) was taken as G_{max} and was used for the representation of G/G_{max} curves.

For the fitting of G/G_{max} curves extracted from the voltage pulses protocol, a Boltzmann equation was used:

$$G/G_{\text{max}} = A2 + (A1 - A2) / (1 + \exp((V_m - V_{1/2}) / dx))$$

where $A2$ is the maximal normalized conductance, $A1$ is the minimal normalized conductance, V_m is the test potential, $V_{1/2}$ is the potential for half-maximal activation and dx is the slope factor.

Conductance–voltage (G – V) curves were constructed from the I–V curves of individual cells by dividing the evoked current by the driving force, according to the following equation:

$$G = I / (V_m - V_{\text{rev}})$$

where V_m is the testing potential and V_{rev} is the reversal potential of the current.

The threshold temperatures were estimated as the first point at which the measured signal (F340/F380 or current) deviated by at least

four times the SD of its baseline. All fittings were carried out with the Levenberg–Marquardt method implemented in the Origin 8.0 software.

Data are reported as mean \pm SEM. When comparing two means, statistical significance ($P < 0.05$) was assessed by Student's two-tailed t test. For multiple comparisons of means, one-way ANOVAs were performed, followed by Bonferroni's post-hoc analysis, using GraphPad Prism version 8.00 for Windows (GraphPad Software). During statistical analysis, normality of the data distribution was determined with the Shapiro–Wilk test. The decision to use parametric or non-parametric statistical tests considered additional factors. Many hypothesis tests, including ANOVA, are robust to violations of the normality assumption if the sample size is large enough. This is the case for most calcium imaging data that have samples >30 . In addition, evaluation of the quantile–quantile (Q–Q) plot provided additional insight on the distribution. For non-parametric analysis we used the Kruskal–Wallis test.

2.12 | Materials

Rapamycin and everolimus (40-O-(2-hydroxyethyl)-rapamycin) were purchased from LC laboratories (Woburn, MA) and prepared in a DMSO stock (50 mM). The required volume for experiments was dissolved in pre-warmed (50°C) control solution. When rapamycin or everolimus, were added to the external solution a white cloud of precipitation appeared and gentle shaking was applied until total dissolution was obtained. Due to its poor solubility in water, a solution of 30- μM rapamycin was the highest concentration tested. In separate experiments, application of vehicle (0.06 %DMSO) did not activate TRPM8 channels.

Menthol (Scharlau, Spain),

(1R,2S,5R)-N-(4-methoxyphenyl)-5-methyl-2-propan-2-ylcyclohexane-1-carboxamide (**WS-12**) was purchased from Tocris Bioscience and a stock solution (20 mM) prepared in DMSO. **AMTB** (N-(3-aminopropyl)-2-[(3-methylphenyl)methoxy]-N-(2-thienylmethyl)benzamide hydrochloride; Tocris), **AITC** (Allyl isocyanate; Sigma), **capsaicin** (8-methyl-N-vanillyl-trans-6-nonenamide; Sigma) were prepared as stocks and stored at -20°C .

2.13 | Nomenclature of targets and ligands

Key protein targets and ligands in this article are hyperlinked to corresponding entries in <http://www.guidetopharmacology.org> and are permanently archived in the Concise Guide to PHARMACOLOGY 2023/24 (Alexander, Fabbro, et al., 2023; Alexander, Mathie, et al., 2023).

3 | RESULTS

3.1 | Rapamycin activates recombinant TRPM8 channels

To investigate the effect of rapamycin on TRPM8 channels, we performed intracellular Ca^{2+} imaging experiments on HEK293 cells

stably expressing rat TRPM8 channels (CR#1 cells) (Brauchi et al., 2004). Rapamycin was applied in independent experiments at four different concentrations (1, 3, 10 and 30 μM) for 150 s. As shown in Figure 1a,b, rapamycin produced a dose-dependent activation of TRPM8 channels with an EC_{50} of $6.5 \pm 1.5 \mu\text{M}$. Rapamycin had poor solubility in aqueous solutions, limiting the maximum concentration that could be tested. At low concentrations, the calcium response evoked by rapamycin had a slow rise and was sustained, while at higher concentrations, rapamycin evoked faster responses that desensitized partially during the time of application (Figure 1a).

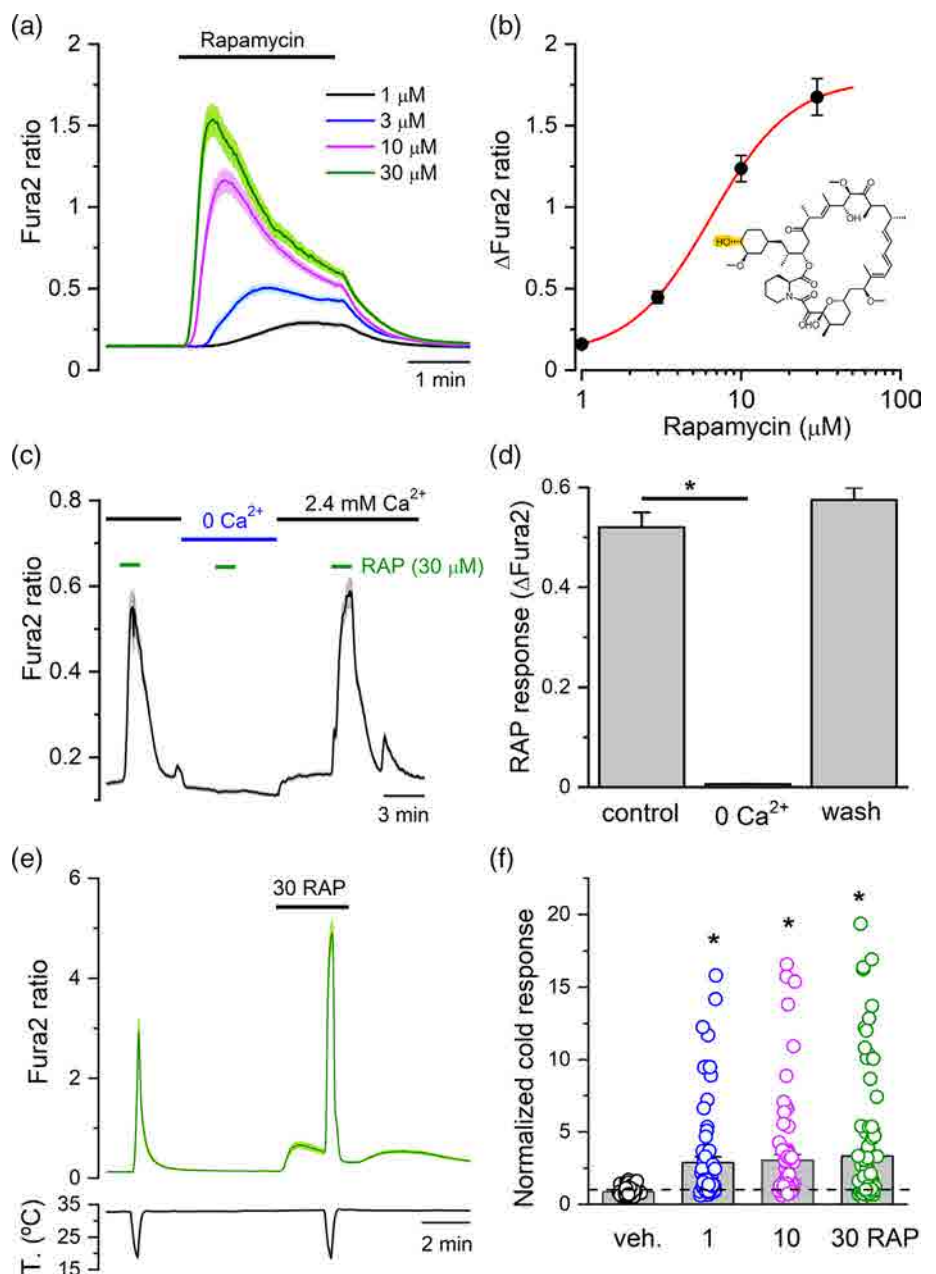
Rapamycin also activates intracellular Ca^{2+} -permeable channels, including TRPML1 at the membrane of lysosomes (Zhang et al., 2019), and ryanodine receptors (RyR) in the endoplasmic reticulum (Brillantes et al., 1994; Lombardi et al., 2017). In order to corroborate

that calcium responses evoked by rapamycin were due to calcium influx from the outside (presumably through TRPM8 channels) and not by calcium release from intracellular stores, the effect of rapamycin was explored in the control (2.4-mM Ca^{2+}) and the calcium-free extracellular solution. During calcium imaging experiments, rapamycin (30 μM) evoked clear responses in the presence of extracellular calcium, whereas, when calcium was removed, rapamycin-evoked responses were absent (Figure 1c,d).

3.2 | Rapamycin sensitizes TRPM8 channels to cold temperatures

TRPM8 channel agonists potentiate responses to cold (Mälkiä et al., 2007; Voets et al., 2004). This was tested in CR#1 cells expressing rat

FIGURE 1 Rapamycin activates recombinant TRPM8 channels and potentiates cold-evoked responses. (a) Average \pm SEM Fura2 ratio time course in HEK293 cells stably expressing rat TRPM8 (CR#1 cells) during application of rapamycin (RAP) at different concentrations. A single dose was applied in individual experiments ($n = 38$ to 185 cells, eight experiments). (b) Dose-response curve of rapamycin effects. Data shown are means \pm SEM obtained from individual peak amplitudes from experiments shown in a. (c) Average \pm SEM Fura2 ratio time course in HEK293 cells stably expressing rat TRPM8 during a protocol in which rapamycin responses were monitored in the presence (2.4-mM Ca^{2+}) and in the absence (0 Ca^{2+}) of extracellular calcium ($n = 103$ cells). (d) Bar histogram summarizing the amplitude \pm SEM of rapamycin responses in the presence and absence of extracellular Ca^{2+} ($n = 257$ cells, five experiments). Data shown are means \pm SEM. * $P < 0.05$, significantly different as indicated; one-way ANOVA for repeated measures followed by Bonferroni post-hoc test. (e) Average \pm SEM Fura2 ratio of cold-evoked responses in CR#1 HEK293 cells in control and 30- μM rapamycin ($n = 98$). (f) Bar histogram summarizing the effect of vehicle or 1-, 10-, 30- μM rapamycin on cold-evoked responses. Individual cold responses have been normalized to the amplitude during the first cold ramp (71 to 92 cells per condition). Ratios > 20 have been excluded from the analysis. Data shown are individual values with means \pm SEM. * $P < 0.05$, significantly different from vehicle; one-way ANOVA followed by Bonferroni post-hoc test.



TRPM8, using a double pulse protocol. As shown in Figure 1e,f, cold-evoked responses were strongly potentiated in the presence of 1- to 30- μ M rapamycin, compared with the response obtained in vehicle.

3.3 | Rapamycin activates different TRPM8 orthologues including human

Next, we studied the sensitivity of other TRPM8 orthologues to rapamycin. Transfected HEK293 cells expressing mouse TRPM8 were activated by a cooling ramp, by subsequent application of rapamycin (30 μ M) and by menthol (30 μ M) (Figure 2a). On average, rapamycin- and menthol-evoked responses were similar in amplitude and significantly smaller when compared with cold-evoked responses (Figure 2b). In the presence of rapamycin or menthol, cold-evoked responses were strongly potentiated (Figure 2b). Additionally, there was a subset of mTRPM8 transfected (i.e., GFP+) cells that did not respond to cold in control conditions but responded to cold in the presence of rapamycin or menthol (Figure 2a, green trace). Cells not expressing mTRPM8 (i.e., those not responding to cold in the presence menthol) did not show changes in intracellular Ca^{2+} levels in the presence of rapamycin either (Figure 2a).

To verify that rapamycin-evoked calcium responses were mediated by TRPM8 channels, we tested the effect of AMTB (10 μ M), a selective TRPM8 channel antagonist (Lashinger et al., 2008). As shown in Figure S1, in the presence of AMTB, rapamycin-evoked calcium responses were strongly suppressed. As expected, cold-evoked calcium responses were also blocked by AMTB.

Next, we explored the sensitivity of human TRPM8 channels to rapamycin. In HEK293 cells transiently expressing hTRPM8, rapamycin (30 μ M) evoked a robust response which was similar in amplitude to the cold-evoked response and significantly larger than the menthol-induced response at the same concentration (Figure 2c, d). hTRPM8-mediated cold-evoked responses were also strongly potentiated by rapamycin and, remarkably, this effect was stronger than the menthol-evoked potentiation (Figure 2c). As in the case of mTRPM8, a subset of cold-insensitive cells in control conditions responded to cold in the presence of rapamycin and menthol (Figure 2c). Cells not expressing hTRPM8 did not show changes in intracellular Ca^{2+} levels in the presence of rapamycin (Figure 2c).

In summary, rapamycin acts as an agonist of rat, mouse and human TRPM8 channels. Like other chemical agonists of TRPM8, rapamycin strongly potentiates the response to cold. In human TRPM8 channels, this effect was more potent for rapamycin than for menthol, the canonical TRPM8 agonist.

3.4 | Rapamycin activates the menthol-insensitive TRPM8 mutant

Previously, we reported that tacrolimus can activate the single-mutant TRPM8 (Y745H) that is insensitive to menthol (Bandell et al., 2006). The same result was obtained with rapamycin. As shown in

Figure 2e,f, rapamycin activated mTRPM8-Y745H and potentiated cold-evoked responses.

3.5 | Everolimus does not activate but sensitizes responses to cold

Everolimus is a rapamycin analogue, with similar immunosuppressant and antiproliferative properties by inhibition of the mTOR kinase (Houghton, 2010). Structurally, the only difference between both molecules is a 2-hydroxyethyl ether substituting for a hydroxy group on the cyclohexyl moiety. In HEK293 cells expressing mouse TRPM8, everolimus (30 μ M) did not produce an increase in calcium but the responses to a cold stimulus were potentiated (Figure S2A,B). Similar results were obtained in cells transfected with human TRPM8 (Figure S2C,D). This behaviour contrasts with the effects of rapamycin, tacrolimus (Arcas et al., 2019) or menthol, suggesting that everolimus is a weaker agonist at TRPM8 channels.

3.6 | Effects of rapamycin on other thermoTRP channels

We and others have shown weak effects of tacrolimus on recombinant TRPA1 channels (Arcas et al., 2019; Kita et al., 2019). Thus, we tested the effects of rapamycin on human TRPA1 channels. As shown in Figure S3A, rapamycin (30 μ M) activated human TRPA1 channels, with a slowly rising $[Ca^{2+}]_i$ response. The activating effects of rapamycin on TRPA1 channels were modest, compared with those produced by its canonical agonist AITC (Figure S3A,C). Only around 60% of the cells that responded to AITC were activated by rapamycin. In contrast, no activating effect of rapamycin was observed on cells expressing human (Figure S3B) or rat TRPV1 channels (not shown), which responded readily to capsaicin.

3.7 | Rapamycin activates TRPM8 currents

Next, we studied the effect of rapamycin on TRPM8 channels by electrophysiological techniques. In whole-cell patch-clamp recordings, application of 30- μ M rapamycin consistently activated whole-cell currents in HEK293 cells expressing mouse TRPM8 (Figure 3a). The current-voltage relationship of the RAP-activated current showed strong outward rectification and a reversal potential close to 0 mV, in line with the known properties of TRPM8 channels (Voets et al., 2004) (Figure 3b). These results confirmed the findings obtained in calcium imaging experiments.

Cold-evoked inward currents, measured at -100 mV, were strongly potentiated in the presence of 30- μ M rapamycin, an effect similar to that produced by menthol at the same concentration. Similar potentiation of cold-evoked currents was observed when measured at $+100$ mV. Moreover, rapamycin and menthol at the same concentration (30 μ M) evoked outward currents of similar amplitude

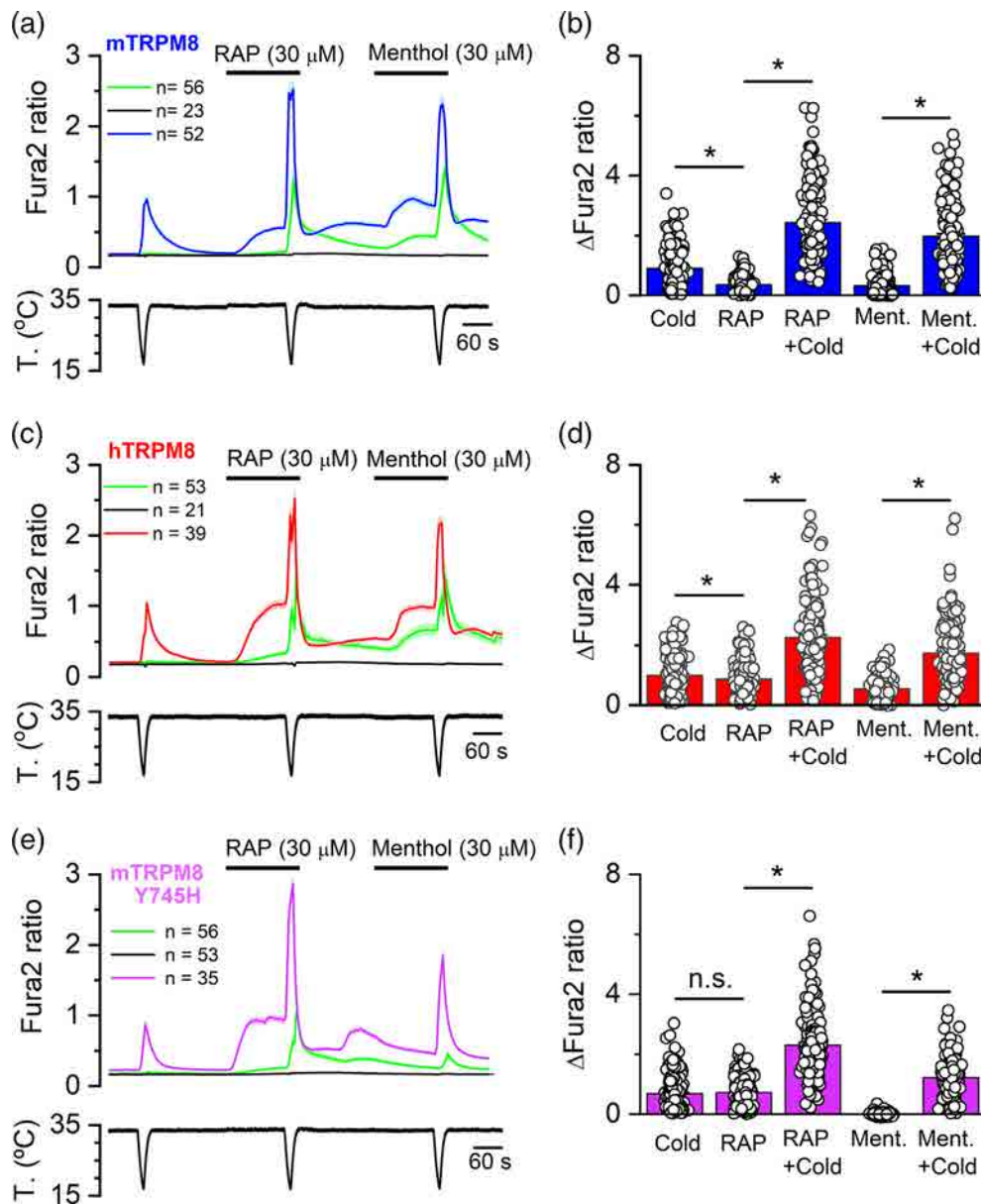


FIGURE 2 Rapamycin activates mouse and human TRPM8 orthologues and the menthol-insensitive mutant. (a) Average \pm SEM Fura2 ratio time course in HEK293 cells expressing mouse TRPM8. Three different behaviours were observed; cells which responded to a first cold ramp in control conditions (blue trace), cells which did not respond to this cold ramp in control conditions but responded to cold in the presence of rapamycin (RAP) or menthol (Ment; green trace), and cells which did not show any response to the applied stimuli (black trace). (b) Bar histogram summarizing the individual and mean responses of the cold-sensitive HEK293 cells ($n = 162$, five experiments). Data shown are individual values with means \pm SEM. * $P < 0.05$, significantly different as indicated; one-way ANOVA followed by Bonferroni post-test. (c) Average \pm SEM Fura2 ratio time course in HEK293 cells expressing human TRPM8. The different traces represented the three behaviours described in a. (d) Bar histogram summarizing the responses of the cold-sensitive HEK293 cells ($n = 178$, five experiments) transfected with human TRPM8. Data shown are individual values with means \pm SEM. * $P < 0.05$, significantly different as indicated; one-way ANOVA followed by Bonferroni post-test. (e) Average \pm SEM Fura2 ratio time course in HEK293 cells expressing mouse TRPM8-Y745H. The different traces represented the three behaviours described in a. (f) Bar histogram summarizing the responses of the cold-sensitive HEK293 cells ($n = 182$, five experiments) transfected with mouse TRPM8-Y745H. Data shown are individual values with means \pm SEM. * $P < 0.05$, significantly different as indicated, n.s., not significant; one-way ANOVA followed by Bonferroni post-test.

suggesting that the potency of both compounds as a TRPM8 channel agonist is similar. A summary of these results is shown in Figure 3c.

To analyse the effects of agonists on voltage-dependent activation of TRPM8 channels, we estimated the $V_{1/2}$ values in the presence of cold, rapamycin and menthol by fitting the traces derived from the voltage ramps with a Boltzmann-linear function (see Section 2) and

compared them to the $V_{1/2}$ value obtained in control conditions at 33°C (Figure 3d). The three agonists produced a notable shift of $V_{1/2}$ towards more negative membrane potentials: Rapamycin and menthol had a similar effect, while cold led to a more pronounced shift, suggesting that it is a stronger agonist. The application of lower concentrations of rapamycin (3 and 10 μ M) induced smaller currents and

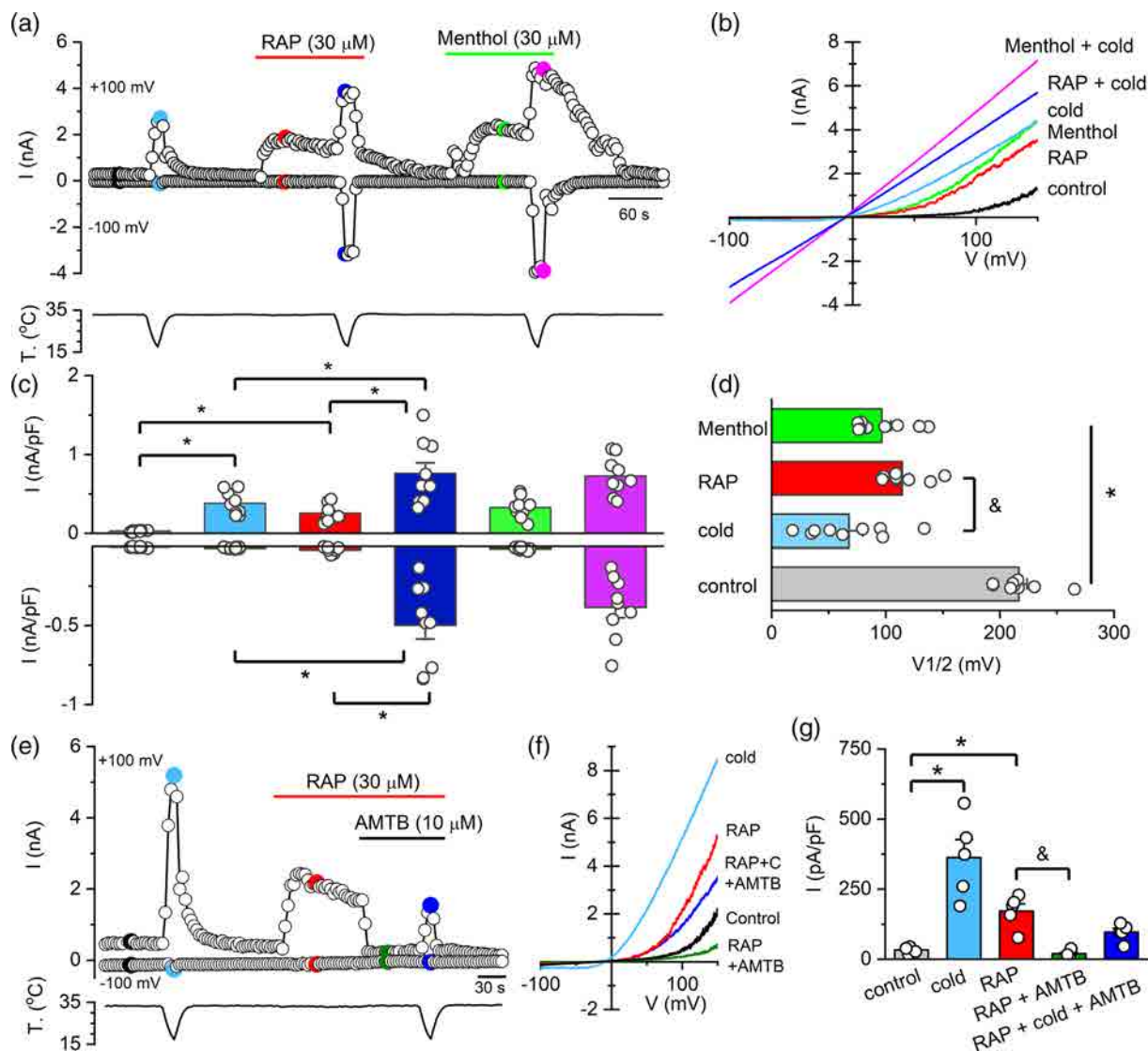


FIGURE 3 Rapamycin (RAP) activates TRPM8 currents. (a) Representative time course of whole-cell current at -100 and $+100$ mV in a HEK293 cell transiently transfected with mTRPM8 during the sequential application of different agonists. The bottom trace shows the simultaneous recording of the bath temperature. (b) Current–voltage (I–V) relationship obtained by a 400-ms voltage ramp from -100 to $+150$ mV during the experiment shown in (a). The colour of individual traces matches the colour at each particular time point in (a). (c) Bar histogram of current density values at -100 and $+100$ mV evoked by the different stimuli shown in (a), with the same colour code ($n = 9$ cells). Data shown are individual values with means \pm SEM. $*P < 0.05$, significantly different as indicated; one-way ANOVA, followed by Bonferroni's post-hoc test. (d) $V_{1/2}$ values calculated from fitting individual I–V curves to a linearized Boltzmann equation. Data shown are individual values with means \pm SEM. $*P < 0.05$, significantly different from control, $\&P < 0.05$, significantly different as indicated; one-way ANOVA, followed by a Bonferroni's post-hoc test. (e) Representative whole-cell current at -100 and $+100$ mV in a HEK293 cell transiently transfected with mTRPM8 during a protocol in which the effect of AMTB on rapamycin response was explored. Bottom trace corresponds to the simultaneous recording of bath temperature. (f) Current–voltage relationship (I–V) obtained with a 400 ms voltage ramp from -100 to $+150$ mV of the responses plotted in e. the colour of the I–V curves matches the coloured time points in e. (g) Bar histogram of individual and mean \pm SEM current density values at $+100$ mV evoked by the different stimuli shown in (e). Data shown are individual values with means \pm SEM; $n = 5$ cells. $*P < 0.05$, significantly different from control, $\&P < 0.05$, significantly different as indicated; one-way ANOVA, followed by Bonferroni's post-hoc test.

smaller shifts in $V_{1/2}$ (Figure S4). These results corroborate that rapamycin, as other TRPM8 channel agonists, activates these channels by a shift in the activation curve towards physiologically relevant membrane potentials.

To confirm the agonist activity of rapamycin on TRPM8 channels, we tested the effect of AMTB, a selective antagonist of these

channels (Lashinger et al., 2008). As shown in Figure 3e,f, AMTB fully suppressed TRPM8 currents evoked by rapamycin. AMTB, at the concentration used ($10 \mu\text{M}$), also blocked the voltage-dependent activation of TRPM8 at the baseline temperature of 33°C (not shown), although it did not totally block the response to cold in the presence of rapamycin (Figure 3e–g).

3.8 | Gating of TRPM8 channels by rapamycin

To characterize the effect of rapamycin on TRPM8 channels at the single channel level, we recorded currents in the cell-attached configuration at room temperature ($\sim 25^{\circ}\text{C}$) in calcium-free, high potassium, extracellular solution (see Section 2). At a fixed voltage (e.g., $+100\text{ mV}$), bath application of $30\text{-}\mu\text{M}$ rapamycin increased channel openings, detected as an increase in the peak current amplitude in the all-point histogram (Figure 4a,b). After washing, the application of $10\text{-}\mu\text{M}$ WS-12 produced openings of similar amplitude. The single channel conductance, estimated from the slope of the I-V relationship of well-resolved openings obtained at different positive membrane potentials was $98.8 \pm 5.9\text{ pS}$ ($n = 14$) in rapamycin (Figure 4c), very similar to the conductance estimate obtained during WS-12 application; $98.6 \pm 10.6\text{ pS}$ ($n = 5$). Reversal potentials measured at the abscissa intercept of current amplitude were $3.2 \pm 3.2\text{ mV}$ in rapamycin and $-3.4 \pm 5.3\text{ mV}$ in WS-12, values consistent with the non-selective nature of the channel (Almaraz et al., 2014; McKemy et al., 2002).

The probability of channel opening induced by rapamycin was voltage dependent, increasing at depolarized potentials (Figure 4d), similar to the effect of WS-12 or other agonists (Zakharian et al., 2010). In the few cases where the patch contained a single channel, the increase in P_o was explained by an increase in mean open time and a decrease in mean close time (not shown).

Overall, these results indicate that rapamycin activates channels with biophysical properties similar to those induced by WS-12, a canonical TRPM8 channel agonist.

3.9 | Rapamycin activates TRPM8 channels in cold-sensitive DRG neurons

To study the effects of rapamycin on TRPM8-expressing sensory neurons, we performed calcium imaging experiments in DRG cultures from TRPM8^{BAC-EYFP} mice (Morenilla-Palao et al., 2014). TRPM8-expressing neurons were identified by their EYFP expression (Figure 5a,b). Nearly all EYFP(+) neurons, 97% (33 out of 34),

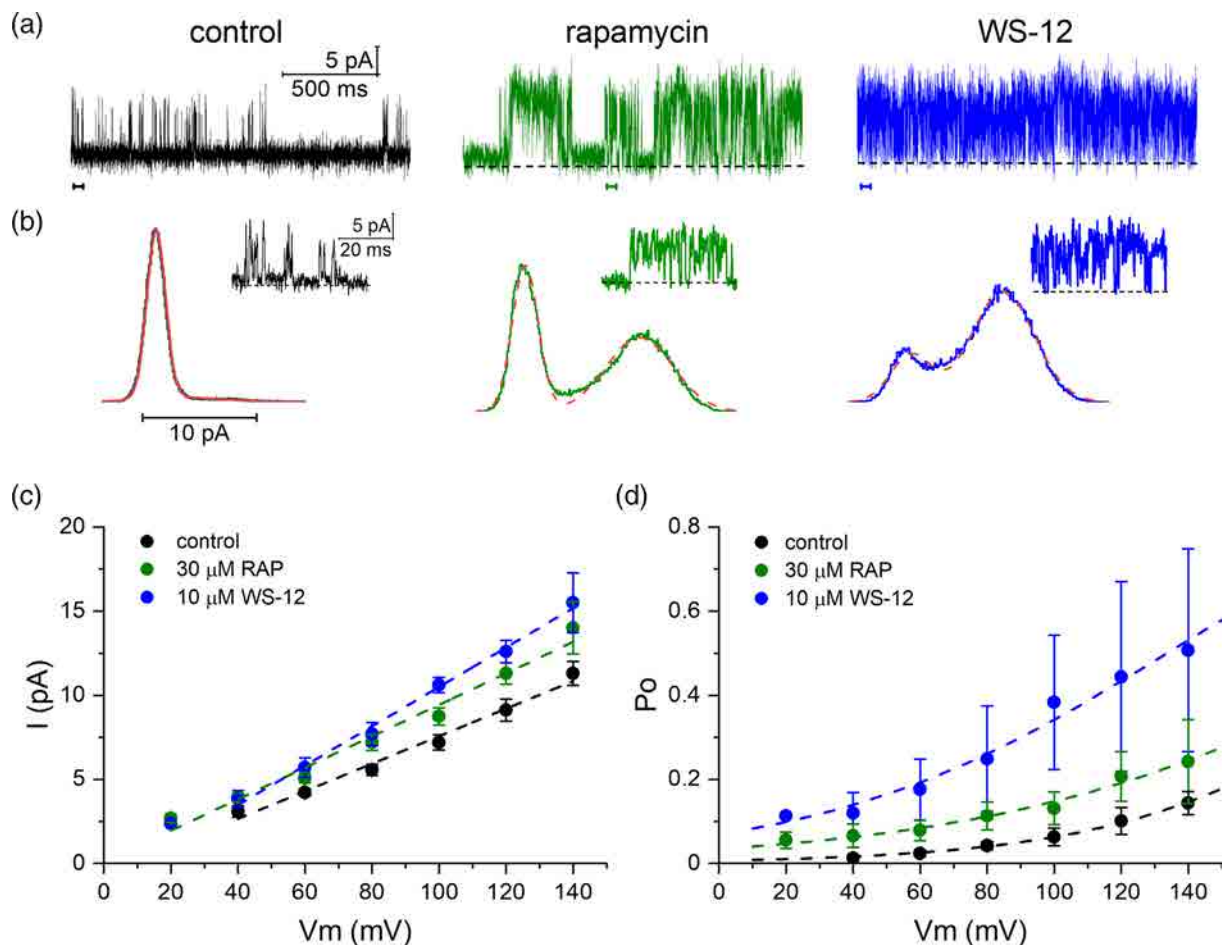


FIGURE 4 Rapamycin activates single TRPM8 channels. (a) Single channel recordings at $+100\text{ mV}$ in the cell-attached configuration in HEK293 cells transfected with mTRPM8. The same patch in control (i.e., high K^+), rapamycin (RAP; $30\text{ }\mu\text{M}$) and WS-12 ($10\text{ }\mu\text{M}$). The coloured ticks mark the expanded traces shown below. (b) All-point histograms of current amplitudes for the different recording conditions. The histograms have been fitted with the sum of two Gaussians (red line). (c) Single channel amplitudes of individual patches at different membrane potentials. The dotted lines represent linear fits to the data. (d) Open probability of channel current at different potentials. The dotted lines are fits to the Boltzmann function.

responded to a cooling ramp and 94.1% (32 out of 34) also responded to rapamycin (30 μ M) application (Figure 5c). In contrast, only a small percentage of EYFP(–) neurons were activated by 30- μ M rapamycin (two out of 236), although they showed normal responses to 30-mM KCl. In agreement with results obtained with recombinant channels, the amplitude of rapamycin-evoked responses was somewhat smaller than cold-evoked responses (Figure 5d). Notably, their respective amplitudes correlated strongly in individual neurons (Figure 5e). The

co-application of a cooling stimulus in the presence of rapamycin produced a marked potentiation in the amplitude of the cold-evoked response (Figure 5d).

To explore the TRPM8-dependence of these responses, we studied a second rapamycin response in the presence of AMTB (10 μ M), a specific blocker of TRPM8 channels (Lashinger et al., 2008). Responses to rapamycin were abolished in the presence of AMTB, confirming the absolute TRPM8 dependence of rapamycin responses

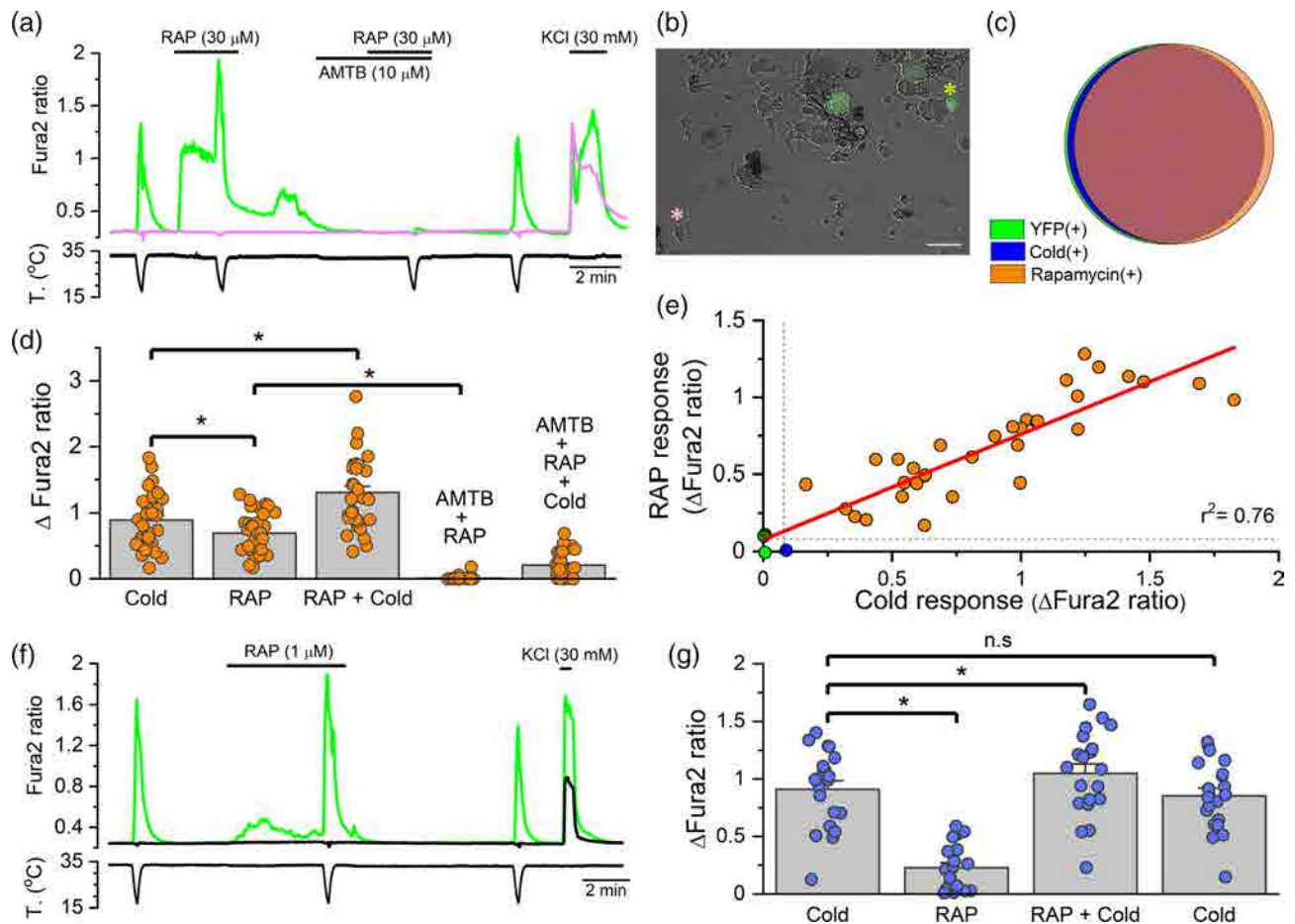


FIGURE 5 Rapamycin (RAP) activates cold-sensitive neurons and potentiates their cold-evoked response. (a) Representative Fura2 fluorescence measurement from cultured DRG neurons in a TRPM8^{BAC-EYFP} mouse. A cold-sensitive and EYFP(+) neuron (green trace) and a EYFP(–) neuron (pink trace) are displayed. Bottom trace corresponds to the simultaneous recording of bath temperature. (b) Superimposed, transmitted and EYFP fluorescence images from DRG cultured neurons of a TRPM8^{BAC-EYFP} mouse. Asterisks correspond to the neurons whose traces are shown in (a). The other two fluorescent neurons in the field had a baseline calcium level higher than 0.8 and were not included in the analysis. The calibration bar is 100 μ m. (c) Venn diagram showing the very strong overlap between EYFP(+) neurons ($n = 34$), cold-sensitive neurons ($n = 33$) and rapamycin-sensitive neurons ($n = 32$). Only two out of 236 EYFP(–) neurons were rapamycin-sensitive. (d) Bar histogram of amplitude responses observed in EYFP(+) rapamycin-sensitive neurons ($n = 32$ neurons, six experiments). Data shown are individual values with means \pm SEM. * $P < 0.05$, significantly different as indicated; one-way ANOVA for repeated measures followed by Bonferroni's post-hoc test. (e) Correlation between amplitude of cold- and rapamycin-evoked responses in individual EYFP(+) DRG neurons ($n = 34$). Orange circles represent neurons that responded to rapamycin and cold, dark blue circle represents the neuron which responded to cold but not to rapamycin (note the very small response to cold), the green circle represents the single EYFP(+) neuron which did not respond to either stimulus and the olive points represent the only two EYFP(–) neurons which respond to rapamycin (overlapped). Dotted lines delimited the threshold that was considered as a response (ΔF_2 ratio = 0.08). (f) Time course of Fura2 ratio of a cold-sensitive EYFP(+) neuron (green trace) in which rapamycin (1 μ M) evoked a substantially increase in intracellular calcium levels, and a cold-insensitive EYFP(–) neuron (black trace). Bottom trace corresponds to the simultaneous recording of bath temperature. (g) Bar histogram summarizing the effect of rapamycin (1 μ M) on cold-sensitive neurons ($n = 20$ neurons, five experiments). Data shown are individual values with means \pm SEM. * $P < 0.05$, significantly different as indicated, n.s., not significant; one-way ANOVA for repeated measures followed by Bonferroni post-hoc test.

in cold-sensitive DRG neurons (Figure 5a,d). The cold-evoked response in the presence of rapamycin was also strongly reduced in the presence of this antagonist, and cold sensitivity recovered after AMTB wash out (Figure 5a,d).

Next, we examined the effect of a lower concentration of rapamycin (1 μ M) on the thermal sensitivity of TRPM8-expressing DRG neurons (Figure 5f). At this lower concentration, rapamycin activated 70% (14 out of 20) of the cold-sensitive, and EYFP(+) neurons tested. Responses were of low amplitude (Figure 5g). However, at this lower concentration, rapamycin significantly potentiated the cold-evoked response in a reversible manner (Figure 5f,g).

Collectively, these results indicated that rapamycin activated cold-sensitive TRPM8-expressing DRG neurons in a highly specific manner. Rapamycin even at low concentrations, strongly potentiated cold-evoked response of these neurons.

3.10 | Rapamycin responses in DRG neurons are mediated by TRPM8 channels

To demonstrate the dependence of rapamycin responses on TRPM8, we took advantage of a transgenic mouse line (*Trpm8*^{EGFPf}) expressing EGFPf from the *Trpm8* locus (Dhaka et al., 2008). Heterozygous mice (*TRPM8*^{EGFPf/+}) in this line express one functional copy of TRPM8 and one copy of EGFPf, while the homozygous littermates (*TRPM8*^{EGFPf/EGFPf}) are KO for TRPM8 channels. In *TRPM8*^{EGFPf/+} DRG cultures, all EGFPf(+) neurons (23 out of 23) responded to a cold ramp in control conditions and to menthol (100 μ M), confirming the expression of TRPM8 channels. They represented 13.9% of all the neurons in the culture. The majority of these TRPM8-expressing neurons, 87% (20 out of 23), also responded to rapamycin (30 μ M) (Figure 6a,b). In contrast, only three out of 140 EGFPf(−) neurons showed a response to rapamycin (Figure 6b), a significantly lower fraction, compared with the EGFPf(+) population. Similar to observations in *TRPM8*^{BAC-EYFP} mice, rapamycin-induced responses were smaller in amplitude than cold-evoked responses, and their amplitudes were correlated in individual neurons (Figure 6d). Rapamycin was also effective in potentiating the cold-evoked response, in line with the effects of the canonical agonist, menthol (Figure 6c).

Confirming previous findings (Arcas et al., 2019; Dhaka et al., 2007), in DRGs from homozygous mice (*Trpm8*^{EGFPf/EGFPf}), the responses to menthol and cold were abrogated; none of the 36 EGFPf(+) recorded neurons responded to 100- μ M menthol and only two of them responded to cold. Rapamycin responses were also very infrequent in these cultures. Only five out of 257 (1.9%) neurons responded to RAP, three were EGFPf(+) and two were EGFPf(−) (Figure 6e,f). This decrease in the percentage of rapamycin responses in EGFPf(+) neurons was highly significant. Interestingly, the responses to rapamycin in these three EGFPf(+) neurons were maintained during the time of application and decreased during the cooling ramp (Figure 6e), while the responses of EGFPf(−) neurons were transient and smaller in amplitude (not shown). Two of these EGFPf(+) RAP-sensitive neurons responded to capsaicin, while the other was

capsaicin-insensitive and AITC-insensitive but was activated by cold and cold in the presence of menthol (not shown).

Altogether, the results obtained in *Trpm8* KO mice indicate that TRPM8 channels mediate the main excitatory action of rapamycin in DRG neurons.

3.11 | Rapamycin activates inward currents and elicits AP firing in TRPM8 cold thermoreceptors

Next, we investigated the effects of rapamycin on cold-sensitive DRG neurons by patch-clamp recordings in cultured neurons from *TRPM8*^{BAC-EYFP} mice. In the whole-cell, voltage-clamp configuration, a cooling ramp in control conditions activated a small inward current (Figure 7a). Application of 30- μ M rapamycin at 33°C also activated a sustained, small inward current and strongly potentiated the cold-evoked response. A summary of these results is shown in Figure 7c. In the presence of rapamycin, the apparent activation of the cold-evoked current shifted to warmer temperatures (Figure 7b). The potentiated currents showed variable degrees of desensitization, likely reflecting the effects of elevated intracellular calcium on TRPM8 gating (Reid et al., 2002; Sarria et al., 2011). In a fraction of neurons, after the rapamycin challenge, we tested the application of menthol (30 μ M), which produced similar effects (Figure S5).

In the current-clamp recording configuration, rapamycin induced the firing of action potentials in cold-sensitive neurons at a basal temperature of 33°C in all the neurons tested (11 out of 11) (Figure 7d,e). The cold- and rapamycin-evoked firing frequency was similar and the combined application of cold and RAP strongly potentiated the firing produced by cold alone (Figure 7e). The duration of firing during the cooling ramp in the presence of agonist was limited by the spike inactivation produced by the strong depolarization (Figure 7d).

These results corroborate that rapamycin is able to trigger a depolarizing current in *TRPM8*(+) cold-sensitive DRG neurons, increasing their excitability to cold temperatures.

3.12 | Rapamycin activates cutaneous cold-sensitive fibres

To characterize the effects of rapamycin on cutaneous cold thermoreceptor endings, we used a mouse skin-nerve preparation of the hind leg (Arcas et al., 2019; Zimmermann et al., 2009), probing the corium surface of the skin with a miniature ice pellet, trying to find unimodal cold receptors (i.e., insensitive to mechanical stimuli) (Toro et al., 2015; Winter et al., 2017). We identified five fibres in the saphenous nerve with such characteristics. These fibres were silent at the baseline temperature of 34–35°C but were activated when cold solution was delivered to their isolated receptive field (Figure 8a,b). During application of rapamycin (30 μ M), all five fibres became spontaneously active at the basal temperature of 34°C. Their cold-evoked activity was clearly modified in the presence of rapamycin, shifting their cold threshold to warmer temperatures (Figure 8c) and shifted

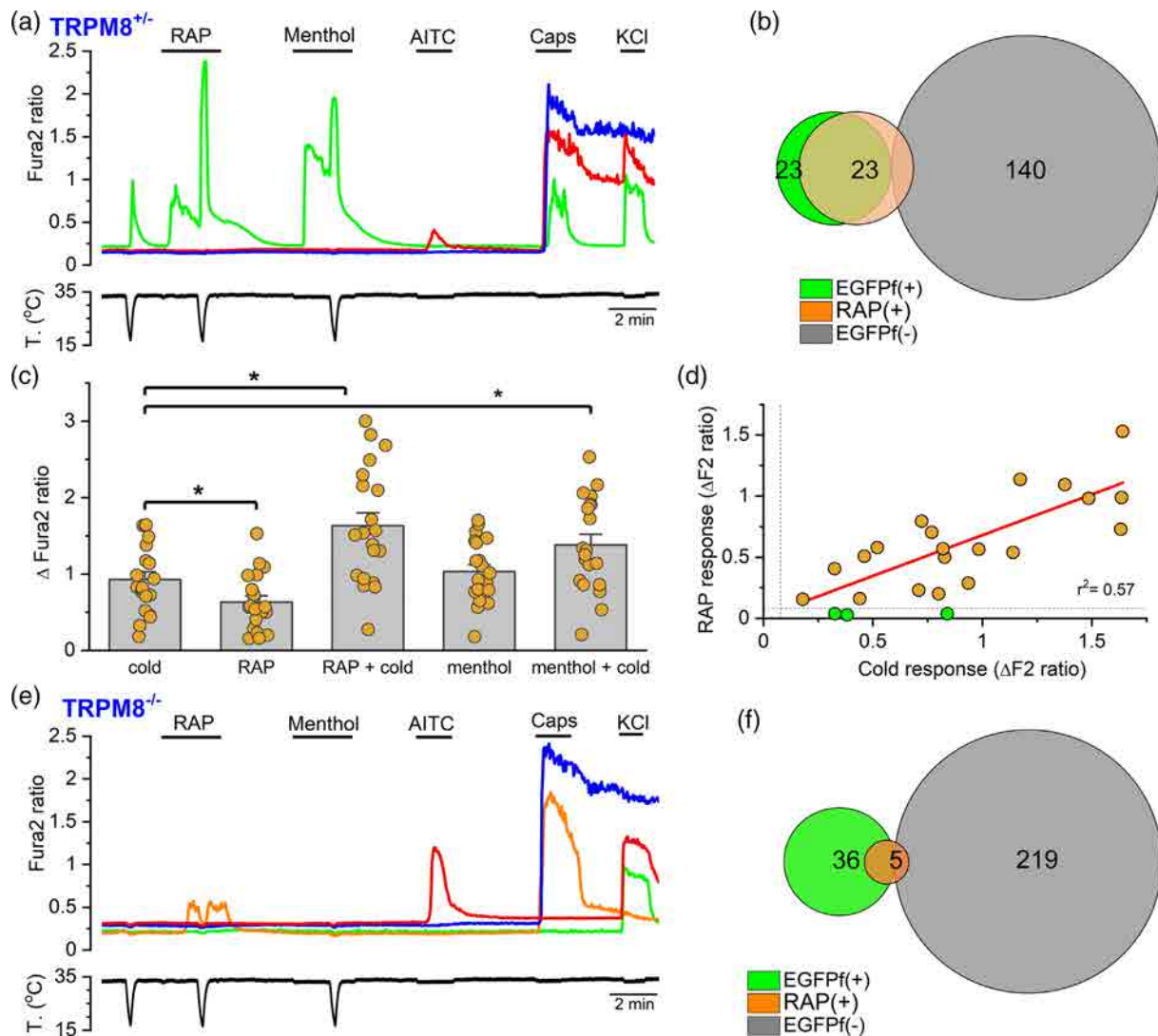


FIGURE 6 TRPM8 is the principal determinant of rapamycin responses in mouse DRG neurons. (a) Representative traces of Fura2 ratio fluorescence in a *Trpm8*^{EGFPf/+} DRG culture. Consecutive applications of cold, rapamycin (RAP, 30 μ M), menthol (100 μ M), AITC (100 μ M), capsaicin (100 nM) and high K⁺ (30 mM) were used to phenotype each neuron. The green trace corresponds to a EGFPf(+) neuron, which responds to cold, rapamycin, menthol and capsaicin. The other two traces (blue and red) correspond to EGFPf(-) neurons. Bottom trace shows the simultaneous recording of bath temperature. (b) Venn diagram summarizing the responses to rapamycin in EGFPf(+) and EGFPf(-) neurons in *Trpm8*^{EGFPf/+} DRG cultures. (c) Bar histograms of the amplitude of the responses to different agonists in EGFPf(+) rapamycin-sensitive neurons (n = 20, five experiments). Data shown are individual values with means \pm SEM. **P* < 0.05, significantly different as indicated; one-way ANOVA for repeated measures followed by a Bonferroni's post-hoc test. (d) Correlation between the amplitude of the cold-evoked response and the rapamycin response (n = 20, six experiments). The horizontal dotted line marks the threshold level for rapamycin sensitivity. Green circles represent the three EGFPf(+), cold-sensitive, rapamycin-insensitive neurons recorded. (e) Representative traces of Fura2 ratios in cultured neurons from *Trpm8* KO mouse. The protocol was the same as in (a). Orange trace corresponds to a EGFPf(+) neuron that was rapamycin-sensitive. Green trace represents a EGFPf(+) neuron which was not sensitive to any of the agonists tested and the red and blue traces are examples of two EGFPf(-) neurons. Bottom trace corresponds to the simultaneous recording of the bath temperature during the experiment. (f) Venn diagram summarizing the responses to rapamycin in EGFPf(+) and EGFPf(-) neurons in *Trpm8*^{EGFPf/EGFPf} DRG cultures (eight experiments).

their stimulus response function to warmer temperatures (Figure 8b), consistent with the results obtained for cold-sensitive DRG neurons. In agreement with the effects observed with tacrolimus (Arcas et al., 2019), the washout of rapamycin effects was only partial (Figure 8c,d). Subsequent application of menthol (50 μ M) produced a reactivation of firing in all the fibres tested.

Collectively, these results indicate that rapamycin sensitizes a population of cutaneous TRPM8-expressing thermoreceptor endings to cold temperature.

3.13 | Mathematical modelling of rapamycin effects on cold thermoreceptor activity

To obtain further insight into the effects of rapamycin on the excitability of cold-sensitive DRG neurons, we implemented the conductance-based mathematical model developed by Olivares et al. (2015). In addition to ion conductances needed for action potential generation, this model incorporates a depolarizing cold- and voltage-dependent current (i.e., TRPM8-like). The effects of rapamycin on

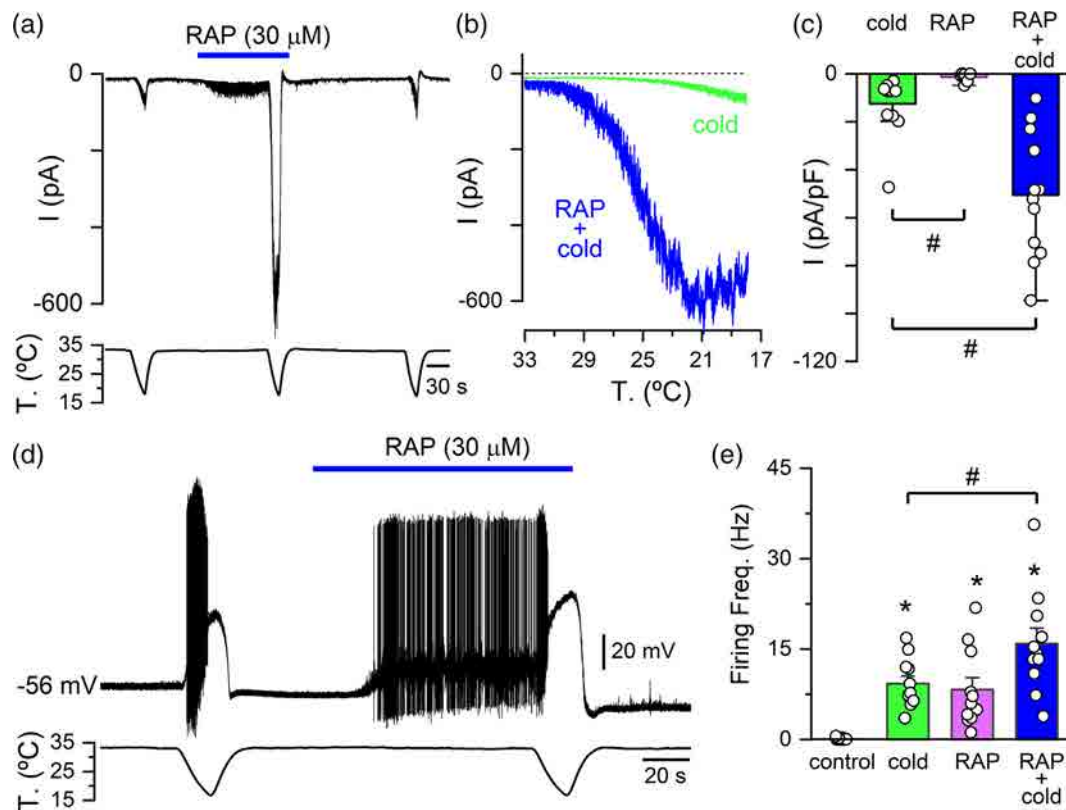


FIGURE 7 Rapamycin (RAP) increases the excitability of cold-sensitive DRG neurons. (a) Representative whole-cell recording in the voltage-clamp configuration ($V_{\text{hold}} = -60$ mV) of a TRPM8-expressing, cold-sensitive DRG neuron identified by EYFP expression. Bottom trace corresponds to the simultaneous recording of bath temperature. Rapamycin activates a small inward current and potentiates the response to cold. (b) Temperature dependence of the cold-evoked current in the same neuron in control conditions and in the presence of 30 μM rapamycin. (c) Bar histogram of peak inward current density values evoked by cold, rapamycin and cold in the presence of rapamycin ($n = 12$). Data shown are individual values with means \pm SEM. $\#P < 0.05$, significantly different as indicated; one-way ANOVA for repeated measures followed by Bonferroni's post-hoc test. (d) Representative recording of a cold-sensitive neuron in the whole-cell current-clamp configuration. Cold and rapamycin elicited the firing of action potentials. The combined application of cold and rapamycin led to faster firing, followed by a strong depolarization and the blockade of spikes. (e) Bar histogram of responses, measured as average firing frequency, during the different stimuli applied ($n = 11$). Firing frequency for cold was the average from the first to the last spike during the cooling ramp. Firing frequency in control conditions was calculated during the 60 s previous to rapamycin application. Rapamycin-evoked firing was calculated from the first spike during rapamycin application to the start of the cold ramp. $*P < 0.05$, significantly different from control, $\#P < 0.05$, significantly different as indicated; one-way ANOVA for repeated measures followed by Bonferroni's post-hoc test.

TRPM8 were simulated as changes in the voltage-dependent activation ($V_{1/2}$) (Voets et al., 2004). We explored the same set of thermosensitive DRG neurons as described in Rivera et al. (2021), including low- and high-threshold neurons (Madrid et al., 2009). Resembling findings observed in culture, simulated neurons showed no spontaneous activity at rest but became vigorously active during cooling ramps (Figure 9a). In current-clamp mode, in the presence of rapamycin the neuron starts firing at the basal temperature, increasing its peak firing frequency further during a second cooling ramp. As shown in Figure 9b,c, changes in $V_{1/2}$ produced graded changes in the temperature threshold and the average firing frequency of low- and high-threshold neurons.

In voltage-clamp mode, application of rapamycin at 34°C produced a modest sustained inward current and a marked increase in peak inward current at the lowest temperature reached (i.e., 18°C) (Figure 9d). Similar to the experimental findings (not shown), the amplitude of the current as a function of temperature presents a

strong hysteresis that is traversed with time in counterclockwise direction (Figure 9e). The increase in cold activated-activated current as a function of rapamycin concentration, modelled as shifts in $V_{1/2}$ ($\Delta V_{1/2} = 0$ mV represents the condition before agonist application) is shown in Figure 9f for six different DRG neurons.

In summary, the experimental effects of rapamycin on cold-thermoreceptor excitability are closely mimicked by effects of rapamycin on TRPM8 channel gating.

3.14 | Rapamycin application to the eye evokes tearing by a TRPM8-dependent mechanism

TRPM8 channels play a major role in basal tearing and blinking (Parra et al., 2010; Quallo et al., 2015), and TRPM8 agonists increase tearing and relieve the symptoms of dry eye (Arcas et al., 2019; Parra et al., 2010; Wirta et al., 2022; Yang et al., 2017).

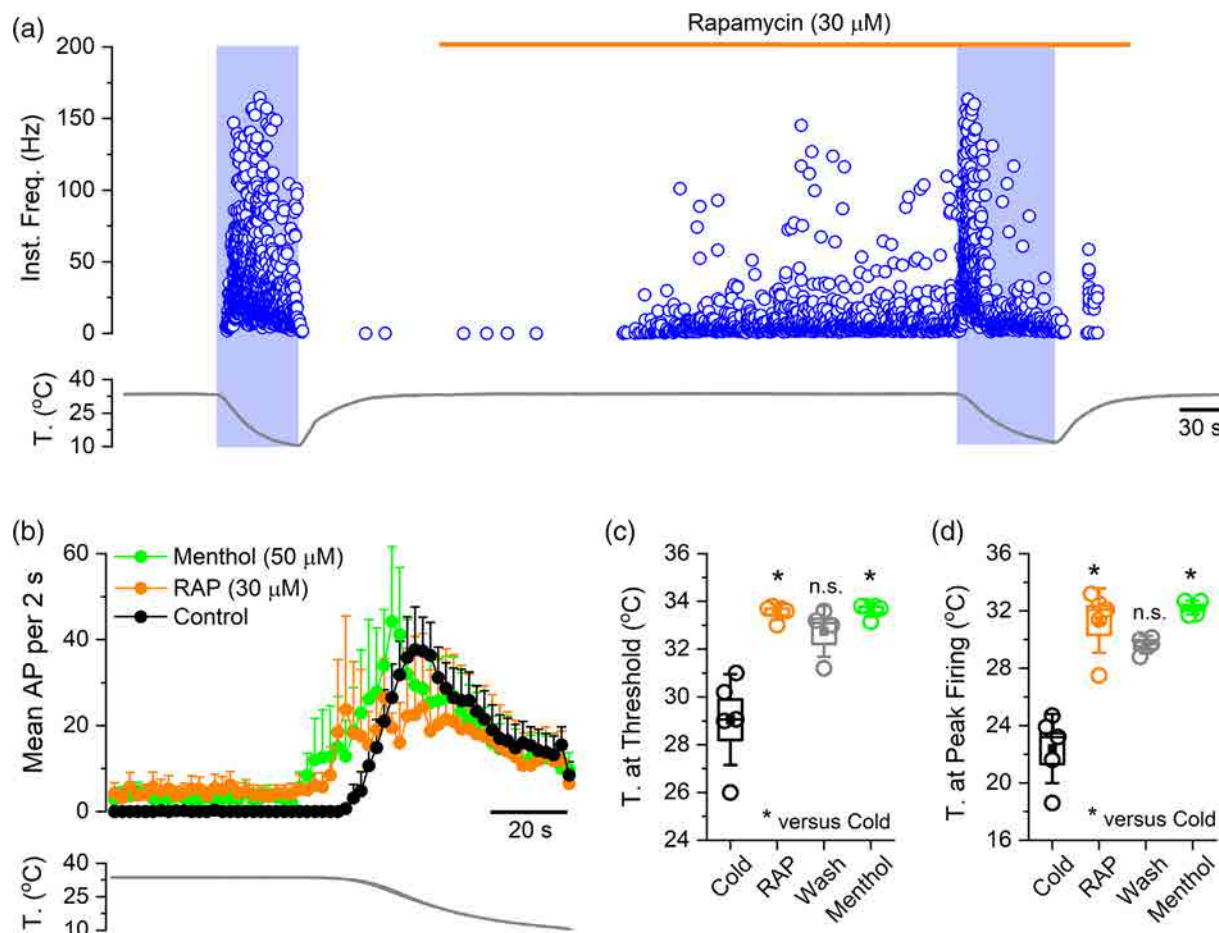


FIGURE 8 Rapamycin activates cutaneous cold-sensitive nerve endings. (a) Representative recording showing the firing response of a single saphenous nerve cold fibre to a decrease in the temperature of the receptive field. The circles represent the instantaneous firing frequency of the fibre. (b) Time course of the averaged cold-evoked response of cold fibres from C57BL/6J mice in control solution, in the presence of 30- μ M rapamycin (RAP) and in 50- μ M menthol. Average discharge rates are represented in bins of 2 s ($n = 5$, five experiments). Bottom, the average temperature ramp for each of the datasets. (c) Temperature threshold for activation of impulse discharge for the different experimental conditions. (d) Temperature at the maximal discharge rate. In (c) and (d), data shown are median values ($n = 5$) with boxes (SEM) and whiskers (SD). * $P < 0.05$, significantly different from Cold, n.s., not significant; Kruskal-Wallis followed by Dunn's test.

We examined the effect of rapamycin solutions on tearing in anaesthetised adult WT mice of both sexes. We applied a small drop of vehicle solution to one eye and measured the tearing after a rest period of 5 min. This was followed by application of 1% rapamycin to the other eye. The experimenter was blind to the solution applied to each eye, and the order of application was also randomized. As shown in Figure 10, in wildtype mice, rapamycin produced a significant increase in tearing compared with vehicle. In contrast, in *Trpm8* KO mice application of rapamycin reduced tearing rate, and the response was similar to the application of vehicle. These results indicate that TRPM8 channels mediate the effects of rapamycin on tearing.

4 | DISCUSSION

Natural products represent a rich resource for modulators of different TRP channels (Julius, 2005; Meotti et al., 2014; Nilius & Appendino, 2011). In the case of TRPM8 channels, menthol, a

monoterpenoid extracted from mint leaves, was crucial for its discovery and functional characterization (McKemy et al., 2002; Peier et al., 2002; Voets et al., 2004). We found that rapamycin, a clinically relevant macrolide immunosuppressant produced by soil microorganisms, and its close analogue everolimus, are novel agonists of TRPM8 channels. They share this property with another macrolide immunosuppressant, tacrolimus (Arcas et al., 2019), generalizing the structure of macrolide rings as chemical activators of TRPM8 channels.

It is noteworthy that rapamycin and tacrolimus (Arcas et al., 2019) can both activate the menthol-insensitive Y745H mutant (Bandell et al., 2006). This result suggests that these macrolides could be binding to the channel at a different site. In this regard, a recent report also described activation of TRPM8 channels by rapamycin in this TRPM8 mutant (Tóth et al., 2024). Moreover, in docking simulations, these authors identified a possible rapamycin binding site of TRPM8, independent of the menthol binding pocket. Additional work, including the screening of additional orthologues and mutagenesis, is currently underway to identify critical residues for rapamycin activation of TRPM8.

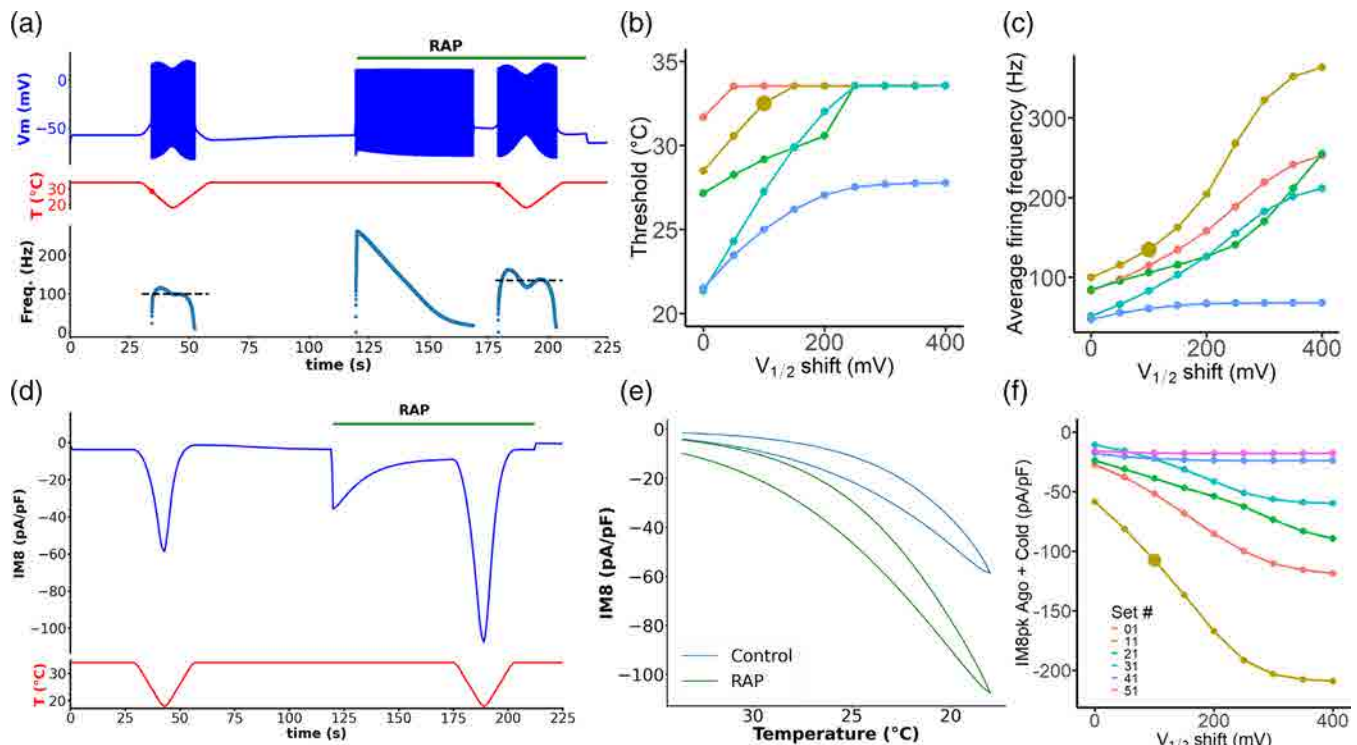


FIGURE 9 Mathematical modelling of the effects of rapamycin (RAP) on cold thermoreceptor activity. (a) Membrane potential (blue trace), temperature (red trace), and action potential firing frequency (blue dots), as a function of time. The green bar indicates the period of application of agonist (i.e. a change of -100 mV in $V_{1/2}$ in this example). The red dots in the temperature trace indicate where the temperature threshold has been reached. The black dashed lines in the lower panel indicate the value of the average firing frequency, and the time range where it has been calculated (i.e. the duration of the temperature ramps). (b) Firing temperature threshold as a function of the shift in $V_{1/2}$. Each trace corresponds to a cell with different parameters, which have been selected in order to encompass a wide range of thresholds under control conditions. The larger dot corresponds to the cell and conditions simulated in panel (a). (c) Same as in panel B for the average firing frequency during cold stimulation. (d) TRPM8 current density (blue trace) as a function of time, and changes in temperature (red trace) in voltage-clamp simulations. The green horizontal bar represents the application of agonist, i.e. a shift of -100 mV in $V_{1/2}$ as in (a). (e) TRPM8 current density as a function of temperature with (green trace) or without agonist (blue trace). (f) Peak cold-evoked current as a function of the shift in $V_{1/2}$ for the same cells as shown above with the corresponding colours. Values for $V_{1/2} = 0$ correspond to the cold-evoked current in the absence of agonist. The magenta line corresponds to a neuron with very small TRPM8 currents that did not fire action potentials and thus is not shown in the current-clamp panels above. Color code is the same for panels b, c, e and f. The set numbers in panel f correspond to the row numbers within the table found in Extended Data Figure 11-1 of Rivera et al. (2021), detailing the simulation parameter values.

Rapamycin potentiates cold-evoked responses by shifting the TRPM8 temperature threshold of activation in a dose-dependent manner, with a clear effect at low micromolar concentrations. Gating effects are similar to those reported for other Type I TRPM8 agonists, including tacrolimus, characterized by the stabilization of the open channel state and a shift in the voltage dependence of activation towards more negative potentials (Janssens et al., 2016). Rapamycin appears to be more potent than tacrolimus, both in recombinant systems and in neurons. For example, in mouse DRG neurons, $1\text{-}\mu\text{M}$ rapamycin produced clear potentiating effects on cold-evoked responses, stronger than those observed with $10\text{-}\mu\text{M}$ tacrolimus (Arcas et al., 2019). Rapamycin-evoked responses are on par to those obtained with the same concentration of menthol, suggesting similar potency as a TRPM8 agonist. In summary, rapamycin activates a depolarizing inward current similar to the TRPM8-dependent I_{Cold} current, increasing the excitability of cold-sensitive DRG neurons.

4.1 | Specificity of rapamycin effects on TRPM8

A recent study found that rapamycin also activates the TRP channel mucolipin 1 (TRPML1) directly, at micromolar concentrations in human fibroblasts (Zhang et al., 2019). This channel is a lysosomal Ca^{2+} -release channel, involved in autophagy. However, multiple lines of evidence suggest that TRPML1 channels are not involved in the responses we observed. First, according to the authors, HEK293 cells (i.e., the heterologous expression system we used) are insensitive to rapamycin (Zhang et al., 2019). Second, our detailed pharmacological characterization of responses in wildtype, hemizygous and TRPM8 KO mice indicates that rapamycin activates TRPM8-expressing sensory neurons in a highly selective manner. Indeed, at the concentration tested, very few rapamycin-responsive cells did not have a TRPM8-like phenotype. In addition, tacrolimus also activates TRPM8 (Arcas et al., 2019) but failed to activate TRPML1 channels (Zhang et al., 2019). Collectively, these results suggest that, in DRG neurons,

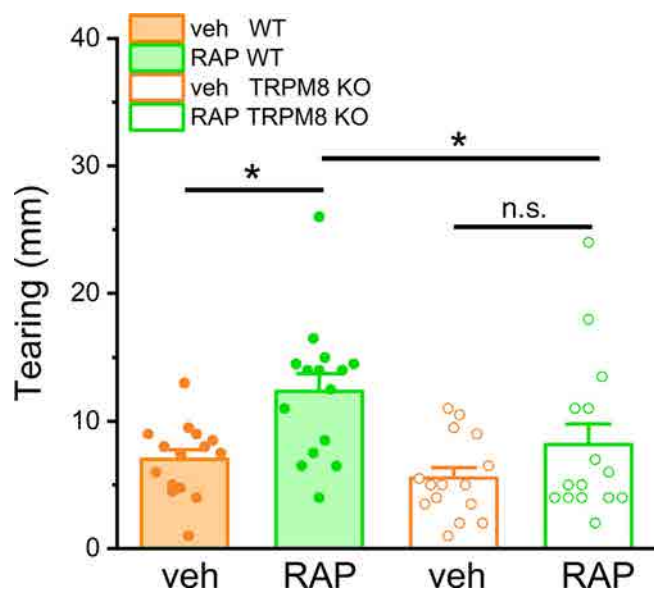


FIGURE 10 Rapamycin stimulates tearing by a TRPM8-dependent mechanism. Effect of topical solutions of rapamycin (RAP; 1%) or vehicle on tearing in mice. Tearing is represented as the length of staining in the threads (in mm) placed in the eye. Each dot corresponds to the tearing measured in an eye of an individual mouse (15 WT and 15 *Trpm8* KO). Data shown are individual values of evoked tearing, with means \pm SEM. * $P < 0.05$, significantly different as indicated; n.s., not significant; Mann-Whitney test).

the effects of rapamycin and other macrolides are mediated by TRPM8 channels. A similar conclusion was reached by Tóth et al. (2024).

In contrast to the very selective effects of rapamycin on TRPM8-expressing mouse sensory neurons, rapamycin also produced a mild activation of human TRPA1 channels overexpressed in HEK293 cells. After topical application of rapamycin for the treatment of facial angiofibromas, patients reported significant skin irritation (Foster et al., 2012; Mutizwa et al., 2011), suggesting that activation of TRPA1 channels may underlie this side effect.

4.2 | Rapamycin as an experimental tool

Rapamycin has been used extensively in cell biology research and other investigations to induce heterodimerization of fusion proteins. This is due to rapamycin's ability to bind with high affinity to FKBP12 and the FRB domain of mTOR, acting as a sort of cell-permeant molecular glue of protein fragments engineered to contain these two domains (Choi et al., 1996; Mangal et al., 2018). Our finding of rapamycin agonistic effect on TRPM8 channels was serendipitous. We were trying to reduce membrane PIP_2 levels with pseudojanin, an enzymatic chimera of inositol polyphosphate 5-phosphatase type IV that depends on rapamycin dimerizing properties for activity (Hammond et al., 2012). Contrary to our expectations, addition of rapamycin to cells expressing pseudojanin did not inhibit TRPM8 channels. Others have used this strategy successfully to investigate

the effects of PIP_2 depletion on TRPM8 channels (Varnai et al., 2006; Zhang, 2019). We suggest an explanation for these divergent results. In the study of Varnai, rapamycin was applied at low concentrations (100 nM) after maximal activation of TRPM8 channels by 500- μ M menthol at room temperature. In contrast, we were working at 34°C and used higher concentrations of rapamycin. It is possible that, under their experimental conditions, the agonist effect of rapamycin is masked by the depletion of PIP_2 induced by the phosphatase. The results obtained in the study by Zhang are more difficult to compare with ours, because he used preincubation of cells with 1- μ M rapamycin, comparing TRPM8 current density with a separate control group.

4.3 | Unexplained effects of rapamycin

Administration of rapamycin has broad effects on the organism biology and some of them are still poorly understood. There is an intriguing connection between rapamycin administration and increased lifespan in several species, including mice (Bitto et al., 2016), but the mechanism is unknown. Interestingly, cold ambient temperature, the physiological agonist of TRPM8 and TRPA1 channels, also increases longevity in many poikilothermic species (Loeb & Northrop, 1916; Xiao et al., 2013). In homeotherms, like mice, the influence of ambient temperature on life span is more complex, due to physiological thermoregulatory mechanisms (Conti, 2008). Nevertheless, in mice with reduced core body temperature, life span is also extended (Conti et al., 2006). Intriguingly, TRPM8 deletion causes lipid accumulation and increased weight in mice (Reimúndez et al., 2018), opposite to the effects of rapamycin treatment (Bitto et al., 2016). Further studies are needed to establish a causal link between rapamycin treatment, TRPM8 activation and extended lifespan. Characterizing the effects of rapamycin treatment on lifespan in TRPM8 KO mice could shed light on the mechanisms involved in life extension.

A known side effect of rapamycin treatment is testicular toxicity, with impaired spermatogenesis and reduced testosterone levels (Rovira et al., 2012). TRPM8 is highly expressed in human and mouse sperm where it participates in different aspects of their physiology (Martínez-López et al., 2011). In light of our findings, and the fact that testosterone is an activator of TRPM8 (Asuthkar et al., 2015), a possible connection between rapamycin and TRPM8 channels in the testis is worth exploring further.

4.4 | Therapeutic implications

TRPM8 channels play different roles in somatosensation, from sensing noxious cold (Knowlton et al., 2013), to participating in menthol (Liu et al., 2013) and cooling-mediated analgesia (Proudfoot et al., 2006), or relieving pruritus (Palkar et al., 2018). TRPM8 is also overexpressed in various types of cancers, including melanoma (Tsavaler et al., 2001). Due to their potential therapeutic benefit, identification of novel TRPM8 modulators (agonists and antagonists) has been in the agenda of many pharmaceutical companies and

academic research groups (Izquierdo et al., 2021; Moran & Szallasi, 2017). Because of severe side effects, it is doubtful that systemic rapamycin will find an application as an anti-inflammatory agent. In contrast, topical applications could be beneficial for different conditions, including ocular pathologies and skin diseases. TRPM8 channels play an important role in the pathophysiology of dry eye disease (DED) (Parra et al., 2010), and several clinical trials have shown that TRPM8 channel agonists can relieve symptoms of ocular discomfort (Wirta et al., 2022; Yang et al., 2017). Our findings suggest that topical application of rapamycin could be a novel treatment for DED by activation of TRPM8 channels. In fact, topical formulations of rapamycin are currently used for the treatment of various ocular disorders in humans and other animals. In particular, it is effective in the treatment of keratoconjunctivitis sicca, a very common disease in dogs, by stimulating tear production (Spatola et al., 2018). In this study, tear production was also increased in control animals, suggesting that the drug has direct lacrimostimulant properties, independently of its anti-inflammatory and immunosuppressive activity. In relation to skin pathologies, TRPM8 is expressed in keratinocytes (Bidaux et al., 2015; Denda et al., 2010) and human melanoma cells (Yamamura et al., 2008). Topical application of TRPM8 agonists accelerates epidermal permeability barrier recovery after injury (Denda et al., 2010). In cultured human melanoma G-361 cells, application of menthol produced a dose-dependent decrease in their viability (Yamamura et al., 2008). Inhibition of mTOR by rapamycin and its analogues continues to be explored as a viable therapy in various cancers (see Zou et al., 2020). Further preclinical studies are required to explore the link between TRPM8 modulation by rapamycin and tumour cell growth.

In conclusion, our findings indicated that rapamycin, a drug already approved for clinical use, may be repurposed for the treatment of pathologies related to TRPM8 channel dysfunction, a concept that is called “drug repositioning” (Doan et al., 2011). This is an interesting strategy in drug discovery, with some important advantages compared with the de novo identification and development of active compounds. Because safety and pharmacokinetic profiles of repositioned candidates are already well established, it allows a dramatic reduction in development time and expense.

In summary, these findings identify rapamycin as a novel TRPM8 agonist and generalize the agonist effects of different macrolide immunosuppressants towards this polymodal ion channel.

AUTHOR CONTRIBUTIONS

A significant fraction of the data presented is part of the PhD Thesis of the first author, José Miguel Arcas, defended at the Universidad Miguel Hernández in 2019, available on-line at <https://dialnet.unirioja.es/servlet/tesis?codigo=221625>. J.M. Arcas, K. Oudaha and J. Castro-Marsal performed patch-clamp recordings and their analysis, J.M. Arcas, K. Oudaha, F. Viana, E. de la Peña and S. Poyraz performed calcium imaging recordings and their analysis, J. Fernández-Trillo and F.A. Peralta performed behavioural experiments and A. Gomis supervised the analysis, A. Gonzalez performed skin nerve recordings and analysis, S. Sala performed computer simulations, S. Sala and E. de la

Peña performed single-channel recordings and their analysis, F. Taberner designed TRPM8 expression plasmids, A. Gomis and F. Viana obtained funding and supervised the project. F. Viana wrote the initial draft of the manuscript. All authors contributed to the writing and revision of the final version of the manuscript.

ACKNOWLEDGEMENTS

We thank Ardem Patapoutian and Ajay Dhaka for providing the *Trpm8*^{EGFPf} mouse line, Patricio Orio for help with computer simulations and Juana Gallar for help with tearing measurements. M. Tora, E. Quintero, R. Torres and the SHARE service IN are acknowledged for excellent technical assistance. During the course of this work, JMA was supported by a predoctoral fellowships from the Spanish Ministry of Education and Science (SO). KO was supported by a fellowship from Generalitat Valenciana (GRISOLIA/2019/089). JC is recipient of a JAE Intro fellowship from CSIC (JAEINT_22_01043). SP was supported by Erasmus+ program of the European Union. The work was funded by Generalitat Valenciana (PROMETEO/2021/03), the International Center for Aging Research (ICAR; project ionRAPA) and the Spanish MCIU/AEI through projects PID2019-108194RB-I00/AEI/10.13039/501100011033, PID20221409610B-I00/AEI/10.13039/501100011033 and Centro de Excelencia Severo Ochoa (CEX2021-001165-S), and co-financed by the European Regional Development Fund (ERDF).

CONFLICT OF INTEREST STATEMENT

The authors declare no conflict of interest.

DATA AVAILABILITY STATEMENT

The data supporting this study's findings, and additional explanations to interpret them, are available from the corresponding author on motivated request.

DECLARATION OF TRANSPARENCY AND SCIENTIFIC RIGOUR

This Declaration acknowledges that this paper adheres to the principles for transparent reporting and scientific rigour of preclinical research as stated in the *BJP* guidelines for [Design and Analysis](#) and [Animal Experimentation](#) and as recommended by funding agencies, publishers and other organizations engaged with supporting research.

ORCID

Khalid Oudaha  <https://orcid.org/0009-0003-8357-2943>
 Alejandro González  <https://orcid.org/0000-0001-7513-2516>
 Jorge Fernández-Trillo  <https://orcid.org/0000-0002-2086-1727>
 Francisco Andrés Peralta  <https://orcid.org/0000-0002-0727-1706>
 Júlia Castro-Marsal  <https://orcid.org/0009-0007-1491-5147>
 Francisco Taberner  <https://orcid.org/0000-0001-5725-6267>
 Salvador Sala  <https://orcid.org/0000-0002-5607-0097>
 Elvira de la Peña  <https://orcid.org/0000-0001-5961-5067>
 Ana Gomis  <https://orcid.org/0000-0003-4651-7673>
 Félix Viana  <https://orcid.org/0000-0003-1439-949X>

REFERENCES

- Alexander, S. P. H., Fabbro, D., Kelly, E., Mathie, A. A., Peters, J. A., Veale, E. L., Armstrong, J. F., Faccenda, E., Harding, S. D., Davies, J. A., Annett, S., Boison, D., Burns, K. E., Dessauer, C., Gertsch, J., Helsby, N. A., Izzo, A. A., Ostrom, R., Papapetropoulos, A., ... Wong, S. S. (2023). The Concise Guide to PHARMACOLOGY 2023/24: Enzymes. *British Journal of Pharmacology*, 180, S289–S373. <https://doi.org/10.1111/bph.16181>
- Alexander, S. P. H., Mathie, A. A., Peters, J. A., Veale, E. L., Striessnig, J., Kelly, E., Armstrong, J. F., Faccenda, E., Harding, S. D., Davies, J. A., Aldrich, R. W., Attali, B., Baggetta, A. M., Becirovic, E., Biel, M., Bill, R. M., Caceres, A. I., Catterall, W. A., Conner, A. C., ... Zhu, M. (2023). The Concise Guide to PHARMACOLOGY 2023/24: Ion channels. *British Journal of Pharmacology*, 180(Suppl 2), S145–S222. <https://doi.org/10.1111/bph.16178>
- Almaraz, L., Manenschijn, J. A., de la Pena, E., & Viana, F. (2014). Trpm8. *Handbook of Experimental Pharmacology*, 222, 547–579. https://doi.org/10.1007/978-3-642-54215-2_22
- Arcas, J. M., González, A., Gers-Barlag, K., González-González, O., Bech, F., Demirkhanyan, L., Zakharian, E., Belmonte, C., Gomis, A., & Viana, F. (2019). The immunosuppressant macrolide tacrolimus activates cold-sensing TRPM8 channels. *The Journal of Neuroscience*, 39(6), 949–969. <https://doi.org/10.1523/JNEUROSCI.1726-18.2018>
- Asuthkar, S., Demirkhanyan, L., Sun, X., Elustondo, P. A., Krishnan, V., Baskaran, P., Velpula, K. K., Thyagarajan, B., Pavlov, E. V., & Zakharian, E. (2015). The TRPM8 protein is a testosterone receptor: II. Functional evidence for an ionotropic effect of testosterone on TRPM8. *The Journal of Biological Chemistry*, 290(5), 2670–2688. <https://doi.org/10.1074/jbc.M114.610873>
- Bandell, M., Dubin, A. E., Petrus, M. J., Orth, A., Mathur, J., Hwang, S. W., & Patapoutian, A. (2006). High-throughput random mutagenesis screen reveals TRPM8 residues specifically required for activation by menthol. *Nature Neuroscience*, 9(4), 493–500. <https://doi.org/10.1038/nn1665>
- Benjamin, D., Colombi, M., Moroni, C., & Hall, M. N. (2011). Rapamycin passes the torch: A new generation of mTOR inhibitors. *Nature Reviews. Drug Discovery*, 10(11), 868–880. <https://doi.org/10.1038/nrd3531>
- Bidaux, G., Borowiec, A. S., Dubois, C., Delcourt, P., Schulz, C., Vanden Abeele, F., Lepage, G., Desruelles, E., Bokhobza, A., Dewailly, E., Slomianny, C., Roudbaraki, M., Héliot, L., Bonnal, J. L., Mauroy, B., Mariot, P., Lecomnier, L., & Prevarskaya, N. (2016). Targeting of short TRPM8 isoforms induces 4TM-TRPM8-dependent apoptosis in prostate cancer cells. *Oncotarget*, 7(20), 29063–29080. <https://doi.org/10.18632/oncotarget.8666>
- Bidaux, G., Borowiec, A. S., Gordienko, D., Beck, B., Shapovalov, G. G., Lecomnier, L., Flourakis, M., Vandenbergh, M., Slomianny, C., Dewailly, E., Delcourt, P., Desruelles, E., Ritaine, A., Polakowska, R., Lesage, J., Chami, M., Skryma, R., & Prevarskaya, N. (2015). Epidermal TRPM8 channel isoform controls the balance between keratinocyte proliferation and differentiation in a cold-dependent manner. *Proceedings of the National Academy of Sciences of the United States of America*, 112(26), E3345–E3354. <https://doi.org/10.1073/pnas.1423357112>
- Bitto, A., Ito, T. K., Pineda, V. V., LeTexier, N. J., Huang, H. Z., Sutliff, E., Tung, H., Vizzini, N., Chen, B., Smith, K., Meza, D., Yajima, M., Beyer, R. P., Kerr, K. F., Davis, D. J., Gillespie, C. H., Snyder, J. M., Treuting, P. M., & Kaeberlein, M. (2016). Transient rapamycin treatment can increase lifespan and healthspan in middle-aged mice. *eLife*, 5, e16351. <https://doi.org/10.7554/eLife.16351>
- Brauchi, S., Orío, P., & Latorre, R. (2004). Clues to understanding cold sensation: Thermodynamics and electrophysiological analysis of the cold receptor TRPM8. *Proceedings of the National Academy of Sciences of the United States of America*, 101(43), 15494–15499. <https://doi.org/10.1073/pnas.0406773101>
- Brillantes, A. B., Ondrias, K., Scott, A., Kobrinsky, E., Ondriašová, E., Moschella, M. C., Jayaraman, T., Landers, M., Ehrlich, B. E., & Marks, A. R. (1994). Stabilization of calcium release channel (ryanodine receptor) function by FK506-binding protein. *Cell*, 77(4), 513–523. [https://doi.org/10.1016/0092-8674\(94\)90214-3](https://doi.org/10.1016/0092-8674(94)90214-3)
- Choi, J., Chen, J., Schreiber, S. L., & Clardy, J. (1996). Structure of the FKBP12-rapamycin complex interacting with the binding domain of human FRAP. *Science*, 273(5272), 239–242. <https://doi.org/10.1126/science.273.5272.239>
- Conti, B. (2008). Considerations on temperature, longevity and aging. *Cellular and Molecular Life Sciences*, 65(11), 1626–1630. <https://doi.org/10.1007/s00018-008-7536-1>
- Conti, B., Sanchez-Alavez, M., Winsky-Sommerer, R., Morale, M. C., Lucero, J., Brownell, S., Fabre, V., Huitron-Resendiz, S., Henriksen, S., Zorrilla, E. P., de Lecea, L., & Bartfai, T. (2006). Transgenic mice with a reduced core body temperature have an increased life span. *Science*, 314(5800), 825–828. <https://doi.org/10.1126/science.1132191>
- Curtis, M. J., Alexander, S. P. H., Cirino, G., George, C. H., Kendall, D. A., Insel, P. A., Izzo, A. A., Ji, Y., Panettieri, R. A., Patel, H. H., Sobey, C. G., Stanford, S. C., Stanley, P., Stefanska, B., Stephens, G. J., Teixeira, M. M., Vergnolle, N., & Ahluwalia, A. (2022). Planning experiments: Updated guidance on experimental design and analysis and their reporting III. *British Journal of Pharmacology*, 179(15), 3907–3913. <https://doi.org/10.1111/bph.15868>
- Denda, M., Tsutsumi, M., & Denda, S. (2010). Topical application of TRPM8 agonists accelerates skin permeability barrier recovery and reduces epidermal proliferation induced by barrier insult: Role of cold-sensitive TRP receptors in epidermal permeability barrier homeostasis. *Experimental Dermatology*, 19(9), 791–795. <https://doi.org/10.1111/j.1600-0625.2010.01154.x>
- Dhaka, A., Earley, T. J., Watson, J., & Patapoutian, A. (2008). Visualizing cold spots: TRPM8-expressing sensory neurons and their projections. *The Journal of Neuroscience*, 28(3), 566–575. <https://doi.org/10.1523/JNEUROSCI.3976-07.2008>
- Dhaka, A., Murray, A. N., Mathur, J., Earley, T. J., Petrus, M. J., & Patapoutian, A. (2007). TRPM8 is required for cold sensation in mice. *Neuron*, 54(3), 371–378. <https://doi.org/10.1016/j.neuron.2007.02.024>
- Foster, R. S., Bint, L. J., & Halbert, A. R. (2012). Topical 0.1% rapamycin for angiofibromas in paediatric patients with tuberous sclerosis: A pilot study of four patients. *The Australasian Journal of Dermatology*, 53(1), 52–56. <https://doi.org/10.1111/j.1440-0960.2011.00837.x>
- Hammond, G. R., Fischer, M. J., Anderson, K. E., Holdich, J., Koteci, A., Balla, T., & Irvine, R. F. (2012). PI4P and PI(4,5)P2 are essential but independent lipid determinants of membrane identity. *Science*, 337(6095), 727–730. <https://doi.org/10.1126/science.1222483>
- Harrison, D. E., Strong, R., Sharp, Z. D., Nelson, J. F., Astle, C. M., Flurkey, K., Nadon, N. L., Wilkinson, J. E., Frenkel, K., Carter, C. S., Pahor, M., Javors, M. A., Fernandez, E., & Miller, R. A. (2009). Rapamycin fed late in life extends lifespan in genetically heterogeneous mice. *Nature*, 460(7253), 392–395. <https://doi.org/10.1038/nature08221>
- Heitman, J., Movva, N. R., & Hall, M. N. (1991). Targets for cell cycle arrest by the immunosuppressant rapamycin in yeast. *Science*, 253(5022), 905–909. <https://doi.org/10.1126/science.1715094>
- Houghton, P. J. (2010). Everolimus. *Clinical Cancer Research*, 16(5), 1368–1372. <https://doi.org/10.1158/1078-0432.CCR-09-1314>
- Izquierdo, C., Martin-Martinez, M., Gomez-Monterrey, I., & Gonzalez-Muniz, R. (2021). TRPM8 channels: Advances in structural studies and pharmacological modulation. *International Journal of Molecular Sciences*, 22(16), 8502. <https://doi.org/10.3390/ijms22168502>
- Janssens, A., Gees, M., Toth, B. I., Ghosh, D., Mulier, M., Vennekens, R., Vriens, J., Talavera, K., & Voets, T. (2016). Definition of two agonist types at the mammalian cold-activated channel TRPM8. *eLife*, 5, e17240. <https://doi.org/10.7554/eLife.17240>
- Johnson, S. C., Rabinovitch, P. S., & Kaeberlein, M. (2013). mTOR is a key modulator of ageing and age-related disease. *Nature*, 493(7432), 338–345. <https://doi.org/10.1038/nature11861>

- Julius, D. (2005). From peppers to peppermints: Natural products as probes of the pain pathway. *Harvey Lectures*, 101, 89–115.
- Kennedy, B. K., & Lamming, D. W. (2016). The mechanistic target of rapamycin: The grand ConducTOR of metabolism and aging. *Cell Metabolism*, 23(6), 990–1003. <https://doi.org/10.1016/j.cmet.2016.05.009>
- Kita, T., Uchida, K., Kato, K., Suzuki, Y., Tominaga, M., & Yamazaki, J. (2019). FK506 (tacrolimus) causes pain sensation through the activation of transient receptor potential ankyrin 1 (TRPA1) channels. *The Journal of Physiological Sciences*, 69(2), 305–316. <https://doi.org/10.1007/s12576-018-0647-z>
- Knowlton, W. M., Palkar, R., Lippoldt, E. K., McCoy, D. D., Baluch, F., Chen, J., & McKemy, D. D. (2013). A sensory-labeled line for cold: TRPM8-expressing sensory neurons define the cellular basis for cold, cold pain, and cooling-mediated analgesia. *The Journal of Neuroscience*, 33(7), 2837–2848. <https://doi.org/10.1523/JNEUROSCI.1943-12.2013>
- Kunz, J., & Hall, M. N. (1993). Cyclosporin A, FK506 and rapamycin: More than just immunosuppression. *Trends in Biochemical Sciences*, 18(9), 334–338. [https://doi.org/10.1016/0968-0004\(93\)90069-Y](https://doi.org/10.1016/0968-0004(93)90069-Y)
- Lashinger, E. S., Steinging, M. S., Hieble, J. P., Leon, L. A., Gardner, S. D., Nagilla, R., Davenport, E. A., Hoffman, B. E., Laping, N. J., & Su, X. (2008). AMTB, a TRPM8 channel blocker: Evidence in rats for activity in overactive bladder and painful bladder syndrome. *American Journal of Physiology. Renal Physiology*, 295(3), F803–F810. <https://doi.org/10.1152/ajprenal.90269.2008>
- Li, J., Kim, S. G., & Blenis, J. (2014). Rapamycin: One drug, many effects. *Cell Metabolism*, 19(3), 373–379. <https://doi.org/10.1016/j.cmet.2014.01.001>
- Lilley, E., Stanford, S. C., Kendall, D. E., Alexander, S. P. H., Cirino, G., Docherty, J. R., George, C. H., Insel, P. A., Izzo, A. A., Ji, Y., Panettieri, R. A., Sobey, C. G., Stefanska, B., Stephens, G., Teixeira, M. M., & Ahluwalia, A. (2020). ARRIVE 2.0 and the British Journal of Pharmacology: Updated guidance for 2020. *British Journal of Pharmacology*, 177, 3611–3616. <https://doi.org/10.1111/bph.15178>
- Liu, B., Fan, L., Balakrishna, S., Sui, A., Morris, J. B., & Jordt, S. E. (2013). TRPM8 is the principal mediator of menthol-induced analgesia of acute and inflammatory pain. *Pain*, 154(10), 2169–2177. <https://doi.org/10.1016/j.pain.2013.06.043>
- Loeb, J., & Northrop, J. H. (1916). Is there a temperature coefficient for the duration of life? *Proceedings of the National Academy of Sciences of the United States of America*, 2(8), 456–457. <https://doi.org/10.1073/pnas.2.8.456>
- Lombardi, A., Trimarco, B., Iaccarino, G., & Santulli, G. (2017). Impaired mitochondrial calcium uptake caused by tacrolimus underlies beta-cell failure. *Cell Communication and Signaling: CCS*, 15(1), 47. <https://doi.org/10.1186/s12964-017-0203-0>
- Madrid, R., de la Pena, E., Donovan-Rodríguez, T., Belmonte, C., & Viana, F. (2009). Variable threshold of trigeminal cold-thermosensitive neurons is determined by a balance between TRPM8 and Kv1 potassium channels. *The Journal of Neuroscience*, 29(10), 3120–3131. <https://doi.org/10.1523/JNEUROSCI.4778-08.2009>
- Malkia, A., Pertusa, M., Fernandez-Ballester, G., Ferrer-Montiel, A., & Viana, F. (2009). Differential role of the menthol-binding residue Y745 in the antagonism of thermally gated TRPM8 channels. *Molecular Pain*, 5, 62. <https://doi.org/10.1186/1744-8069-5-62>
- Mangal, S., Zielich, J., Lambie, E., & Zanin, E. (2018). Rapamycin-induced protein dimerization as a tool for *C. elegans* research. *Micropublication Biology*, 2018, W2BH3H. <https://doi.org/10.17912/W2BH3H>
- Martínez-López, P., Treviño, C. L., de la Vega-Beltrán, J. L., de Blas, G., Monroy, E., Beltrán, C., Orta, G., Gibbs, G. M., O'Bryan, M. K., & Darszon, A. (2011). TRPM8 in mouse sperm detects temperature changes and may influence the acrosome reaction. *Journal of Cellular Physiology*, 226(6), 1620–1631. <https://doi.org/10.1002/jcp.22493>
- McKemy, D. D., Neuhausser, W. M., & Julius, D. (2002). Identification of a cold receptor reveals a general role for TRP channels in thermosensation. *Nature*, 416(6876), 52–58. <https://doi.org/10.1038/nature719>
- Meotti, F. C., Lemos de Andrade, E., & Calixto, J. B. (2014). TRP modulation by natural compounds. *Handbook of Experimental Pharmacology*, 223, 1177–1238. https://doi.org/10.1007/978-3-319-05161-1_19
- Moran, M. M., & Szallasi, A. (2017). Targeting nociceptive transient receptor potential channels to treat chronic pain: Current state of the field. *British Journal of Pharmacology*, 175, 2185–2203. <https://doi.org/10.1111/bph.14044>
- Morenilla-Palao, C., Luis, E., Fernandez-Pena, C., Quintero, E., Weaver, J. L., Bayliss, D. A., & Viana, F. (2014). Ion channel profile of TRPM8 cold receptors reveals a role of TASK-3 potassium channels in thermosensation. *Cell Reports*, 8(5), 1571–1582. <https://doi.org/10.1016/j.celrep.2014.08.003>
- Mutizwa, M. M., Berk, D. R., & Anadkat, M. J. (2011). Treatment of facial angiofibromas with topical application of oral rapamycin solution (1mg/mL(-1)) in two patients with tuberous sclerosis. *The British Journal of Dermatology*, 165(4), 922–923. <https://doi.org/10.1111/j.1365-2133.2011.10476.x>
- Nilius, B., & Appendino, G. (2011). Tasty and healthy TR(i)Ps. The human quest for culinary pungency. *EMBO Reports*, 12(11), 1094–1101. <https://doi.org/10.1038/embor.2011.200>
- Olivares, E., Salgado, S., Maidana, J. P., Herrera, G., Campos, M., Madrid, R., & Orio, P. (2015). TRPM8-dependent dynamic response in a mathematical model of cold thermoreceptor. *PLoS ONE*, 10(10), e0139314. <https://doi.org/10.1371/journal.pone.0139314>
- Palkar, R., Ongun, S., Catich, E., Li, N., Borad, N., Sarkisian, A., & McKemy, D. D. (2018). Cooling relief of acute and chronic itch requires TRPM8 channels and neurons. *The Journal of Investigative Dermatology*, 138(6), 1391–1399. <https://doi.org/10.1016/j.jid.2017.12.025>
- Parra, A., Madrid, R., Echevarria, D., del Olmo, S., Morenilla-Palao, C., Acosta, M. C., Gallar, J., Dhaka, A., Viana, F., & Belmonte, C. (2010). Ocular surface wetness is regulated by TRPM8-dependent cold thermoreceptors of the cornea. *Nature Medicine*, 16(12), 1396–1399. <https://doi.org/10.1038/nm.2264>
- Peier, A. M., Moqrich, A., Hergarden, A. C., Reeve, A. J., Andersson, D. A., Story, G. M., Earley, T. J., Dragoni, I., McIntyre, P., Bevan, S., & Patapoutian, A. (2002). A TRP channel that senses cold stimuli and menthol. *Cell*, 108(5), 705–715. [https://doi.org/10.1016/s0092-8674\(02\)00652-9](https://doi.org/10.1016/s0092-8674(02)00652-9)
- Percie du Sert, N., Hurst, V., Ahluwalia, A., Alam, S., Avey, M. T., Baker, M., Browne, W. J., Clark, A., Cuthill, I. C., Dirnagl, U., Emerson, M., Garner, P., Holgate, S. T., Howells, D. W., Karp, N. A., Lasic, S. E., Lidster, K., MacCallum, C. J., Macleod, M., ... Würbel, H. (2020). The ARRIVE guidelines 2.0: updated guidelines for reporting animal research. *PLoS Biol*, 18, e3000410. <https://doi.org/10.1371/journal.pbio.3000410>
- Proudfoot, C. J., Garry, E. M., Cottrell, D. F., Rosie, R., Anderson, H., Robertson, D. C., Fleetwood-Walker, S. M., & Mitchell, R. (2006). Analgesia mediated by the TRPM8 cold receptor in chronic neuropathic pain. *Current Biology*, 16(16), 1591–1605. <https://doi.org/10.1016/j.cub.2006.07.061>
- Quallo, T., Vastani, N., Horridge, E., Gentry, C., Parra, A., Moss, S., Viana, F., Belmonte, C., Andersson, D. A., & Bevan, S. (2015). TRPM8 is a neuronal osmosensor that regulates eye blinking in mice. *Nature Communications*, 6, 7150. <https://doi.org/10.1038/ncomms8150>
- Reid, G., Amuzescu, B., Zech, E., & Flonta, M. L. (2001). A system for applying rapid warming or cooling stimuli to cells during patch clamp recording or ion imaging. *Journal of Neuroscience Methods*, 111(1), 1–8. [https://doi.org/10.1016/S0165-0270\(01\)00416-2](https://doi.org/10.1016/S0165-0270(01)00416-2)
- Reid, G., Babes, A., & Pluteanu, F. (2002). A cold- and menthol-activated current in rat dorsal root ganglion neurones: Properties and role in cold transduction. *The Journal of Physiology*, 545(2), 595–614. <https://doi.org/10.1113/jphysiol.2002.024331>

- Reimúndez, A., Fernández-Peña, C., García, G., Fernández, R., Ordás, P., Gallego, R., Pardo-Vazquez, J. L., Arce, V., Viana, F., & Señañis, R. (2018). Deletion of the cold thermoreceptor TRPM8 increases heat loss and food intake leading to reduced body temperature and obesity in mice. *The Journal of Neuroscience*, 38(15), 3643–3656. <https://doi.org/10.1523/JNEUROSCI.3002-17.2018>
- Rivera, B., Moreno, C., Lavanderos, B., Hwang, J. Y., Fernández-Trillo, J., Park, K. S., Orío, P., Viana, F., Madrid, R., & Pertusa, M. (2021). Constitutive phosphorylation as a key regulator of TRPM8 channel function. *The Journal of Neuroscience*, 41(41), 8475–8493. <https://doi.org/10.1523/JNEUROSCI.0345-21.2021>
- Rovira, J., Diekmann, F., Ramirez-Bajo, M. J., Banon-Maneus, E., Moya-Rull, D., & Campistol, J. M. (2012). Sirolimus-associated testicular toxicity: Detrimental but reversible. *Transplantation*, 93(9), 874–879. <https://doi.org/10.1097/TP.0b013e31824bf1f0>
- Roza, C., Belmonte, C., & Viana, F. (2006). Cold sensitivity in axotomized fibers of experimental neuromas in mice. *Pain*, 120(1–2), 24–35. <https://doi.org/10.1016/j.pain.2005.10.006>
- Sarria, I., Ling, J., Zhu, M. X., & Gu, J. G. (2011). TRPM8 acute desensitization is mediated by calmodulin and requires PIP(2): Distinction from tachyphylaxis. *Journal of Neurophysiology*, 106(6), 3056–3066. <https://doi.org/10.1152/jn.00544.2011>
- Saxton, R. A., & Sabatini, D. M. (2017). mTOR signaling in growth, metabolism, and disease. *Cell*, 168(6), 960–976. <https://doi.org/10.1016/j.cell.2017.02.004>
- Seto, B. (2012). Rapamycin and mTOR: A serendipitous discovery and implications for breast cancer. *Clinical and Translational Medicine*, 1(1), 29. <https://doi.org/10.1186/2001-1326-1-29>
- Spatola, R., Nadelstein, B., Berdoulay, A., & English, R. V. (2018). The effects of topical aqueous sirolimus on tear production in normal dogs and dogs with refractory dry eye. *Veterinary Ophthalmology*, 21(3), 255–263. <https://doi.org/10.1111/vop.12503>
- Takashima, Y., Daniels, R. L., Knowlton, W., Teng, J., Liman, E. R., & McKemy, D. D. (2007). Diversity in the neural circuitry of cold sensing revealed by genetic axonal labeling of transient receptor potential melastatin 8 neurons. *The Journal of Neuroscience*, 27(51), 14147–14157. <https://doi.org/10.1523/JNEUROSCI.4578-07.2007>
- Toro, C. A., Eger, S., Veliz, L., Sotelo-Hitschfeld, P., Cabezas, D., Castro, M. A., Zimmermann, K., & Brauchi, S. (2015). Agonist-dependent modulation of cell surface expression of the cold receptor TRPM8. *The Journal of Neuroscience*, 35(2), 571–582. <https://doi.org/10.1523/JNEUROSCI.3820-13.2015>
- Tóth, B. I., Bazeli, B., Janssens, A., Lisztes, E., Racskó, M., Kelemen, B., Herczeg, M., Nagy, T. M., Kövér, K. E., Mitra, A., Borics, A., & Voets, T. (2024). Direct modulation of TRPM8 ion channels by rapamycin and analog macrolide immunosuppressants. *bioRxiv*, 2024.2002.2001.578392. <https://doi.org/10.1101/2024.02.01.578392>
- Tsavaler, L., Shapero, M. H., Morkowski, S., & Laus, R. (2001). Trp-p8, a novel prostate-specific gene, is up-regulated in prostate cancer and other malignancies and shares high homology with transient receptor potential calcium channel proteins. *Cancer Research*, 61(9), 3760–3769.
- van Unen, J., Rashidfarrokhi, A., Hoogendoorn, E., Postma, M., Gadella, T. W. Jr., & Goedhart, J. (2016). Quantitative single-cell analysis of signaling pathways activated immediately downstream of histamine receptor subtypes. *Molecular Pharmacology*, 90(3), 162–176. <https://doi.org/10.1124/mol.116.104505>
- Varnai, P., Thyagarajan, B., Rohacs, T., & Balla, T. (2006). Rapidly inducible changes in phosphatidylinositol 4,5-bisphosphate levels influence multiple regulatory functions of the lipid in intact living cells. *The Journal of Cell Biology*, 175(3), 377–382. <https://doi.org/10.1083/jcb.200607116>
- Vezina, C., Kudelski, A., & Sehgal, S. N. (1975). Rapamycin (AY-22,989), a new antifungal antibiotic. I. Taxonomy of the producing streptomycete and isolation of the active principle. *Journal of Antibiotics (Tokyo)*, 28(10), 721–726. <https://doi.org/10.7164/antibiotics.28.721>
- Voets, T., Droogmans, G., Wissenbach, U., Janssens, A., Flockerzi, V., & Nilius, B. (2004). The principle of temperature-dependent gating in cold- and heat-sensitive TRP channels. *Nature*, 430(7001), 748–754. <https://doi.org/10.1038/nature02732>
- Wilkinson, J. E., Burmeister, L., Brooks, S. V., Chan, C. C., Friedline, S., Harrison, D. E., Hejtmancik, J. F., Nadon, N., Strong, R., Wood, L. K., Woodward, M. A., & Miller, R. A. (2012). Rapamycin slows aging in mice. *Aging Cell*, 11(4), 675–682. <https://doi.org/10.1111/j.1474-9726.2012.00832.x>
- Winter, Z., Gruschwitz, P., Eger, S., Touska, F., & Zimmermann, K. (2017). Cold temperature encoding by cutaneous TRPA1 and TRPM8-carrying fibers in the mouse. *Frontiers in Molecular Neuroscience*, 10, 209. <https://doi.org/10.3389/fnmol.2017.00209>
- Wirta, D. L., Senchyna, M., Lewis, A. E., Evans, D. G., McLaurin, E. B., Ousler, G. W., & Hollander, D. A. (2022). A randomized, vehicle-controlled, phase 2b study of two concentrations of the TRPM8 receptor agonist AR-15512 in the treatment of dry eye disease (COMET-1). *The Ocular Surface*, 26, 166–173. <https://doi.org/10.1016/j.jtos.2022.08.003>
- Xiao, R., Zhang, B., Dong, Y., Gong, J., Xu, T., Liu, J., & Xu, X. Z. (2013). A genetic program promotes *C. elegans* longevity at cold temperatures via a thermosensitive TRP channel. *Cell*, 152(4), 806–817. <https://doi.org/10.1016/j.cell.2013.01.020>
- Yamamura, H., Ugawa, S., Ueda, T., Morita, A., & Shimada, S. (2008). TRPM8 activation suppresses cellular viability in human melanoma. *American Journal of Physiology. Cell Physiology*, 295(2), C296–C301. <https://doi.org/10.1152/ajpcell.00499.2007>
- Yang, J. M., Li, F., Liu, Q., Rüedi, M., Wei, E. T., Lentsman, M., Lee, H. S., Choi, W., Kim, S. J., & Yoon, K. C. (2017). A novel TRPM8 agonist relieves dry eye discomfort. *BMC Ophthalmology*, 17(1), 101. <https://doi.org/10.1186/s12886-017-0495-2>
- Zakharian, E., Cao, C., & Rohacs, T. (2010). Gating of transient receptor potential melastatin 8 (TRPM8) channels activated by cold and chemical agonists in planar lipid bilayers. *The Journal of Neuroscience*, 30(37), 12526–12534. <https://doi.org/10.1523/JNEUROSCI.3189-10.2010>
- Zakharian, E., Thyagarajan, B., French, R. J., Pavlov, E., & Rohacs, T. (2009). Inorganic polyphosphate modulates TRPM8 channels. *PLoS ONE*, 4(4), e5404. <https://doi.org/10.1371/journal.pone.0005404>
- Zhang, L., & Barritt, G. J. (2006). TRPM8 in prostate cancer cells: A potential diagnostic and prognostic marker with a secretory function? *Endocrine-Related Cancer*, 13(1), 27–38. <https://doi.org/10.1677/erc.1.01093>
- Zhang, X. (2019). Direct Galphaq gating is the sole mechanism for TRPM8 inhibition caused by bradykinin receptor activation. *Cell Reports*, 27(12), 3672–3683.e4. <https://doi.org/10.1016/j.celrep.2019.05.080>
- Zhang, X., Chen, W., Gao, Q., Yang, J., Yan, X., Zhao, H., Su, L., Yang, M., Gao, C., Yao, Y., Inoki, K., Li, D., Shao, R., Wang, S., Sahoo, N., Kudo, F., Eguchi, T., Ruan, B., & Xu, H. (2019). Rapamycin directly activates lysosomal mucolipin TRP channels independent of mTOR. *PLoS Biology*, 17(5), e3000252. <https://doi.org/10.1371/journal.pbio.3000252>
- Zimmermann, K., Hein, A., Hager, U., Kaczmarek, J. S., Turnquist, B. P., Clapham, D. E., & Reeh, P. W. (2009). Phenotyping sensory nerve endings in vitro in the mouse. *Nature Protocols*, 4(2), 174–196. <https://doi.org/10.1038/nprot.2008.223>
- Zou, Z., Tao, T., Li, H., & Zhu, X. (2020). mTOR signaling pathway and mTOR inhibitors in cancer: Progress and challenges. *Cell & Bioscience*, 10, 31. <https://doi.org/10.1186/s13578-020-00396-1>
- Carnevale, T., & Hines, M. (2006). *The NEURON book*. Cambridge University Press.
- Hines, M. L., Davison, A. P., & Muller, E. (2009). NEURON and Python. *Frontiers in Neuroinformatics*, 3, 1. <https://doi.org/10.3389/NEURO.11.001.2009/BIBTEX>

- Harris, C. R., Millman, K. J., van der Walt, S. J., Gommers, R., Virtanen, P., Cournapeau, D., Wieser, E., Taylor, J., Berg, S., Smith, N. J., Kern, R., Picus, M., Hoyer, S., van Kerkwijk, M. H., Brett, M., Haldane, A., Fernández del Río, J., Wiebe, M., Peterson, P., ... Oliphant, T. E. (2020). Array programming with NumPy. *Nature*, 585, 357–362. <https://doi.org/10.1038/s41586-020-2649-2>
- Virtanen, P., Gommers, R., Oliphant, T. E., Haberland, M., Reddy, T., Cournapeau, D., Burovski, E., Peterson, P., Weckesser, W., Bright, J., van der Walt, S. J., Brett, M., Wilson, J., Millman, K. J., Mayorov, N., Nelson, A. R. J., Jones, E., Kern, R., Larson, E., ... SciPy 1.0 Contributors. (2020). SciPy 1.0: Fundamental algorithms for scientific computing in Python. *Nature Methods*, 17, 261–272. <https://doi.org/10.1038/s41592-019-0686-2>
- Hunter, J. D. (2007). Matplotlib: A 2D graphics environment. *Computing in Science & Engineering*, 9(3), 90–95.
- Mälkiä, A., Madrid, R., Meseguer, V., de la Peña, E., Valero, M., Belmonte, C., & Viana, F. (2007). Bidirectional shifts of TRPM8 channel gating by temperature and chemical agents modulate the cold sensitivity of mammalian thermoreceptors. *The Journal of Physiology*, 581(Pt 1), 155–174. <https://doi.org/10.1113/jphysiol.2006.123059>
- Doan, T. L., Pollastri, M., Walters, M. A., & Georg, G. I. (2011). Chapter 23—The future of drug repositioning: Old drugs, new opportunities. In

J. E. Macor (Ed.), *Annual reports in medicinal chemistry* (Vol. 46) (pp. 385–401). Academic Press. <https://doi.org/10.1016/B978-0-12-386009-5.00004-7>

SUPPORTING INFORMATION

Additional supporting information can be found online in the Supporting Information section at the end of this article.

How to cite this article: Arcas, J. M., Oudaha, K., González, A., Fernández-Trillo, J., Peralta, F. A., Castro-Marsal, J., Poyraz, S., Taberner, F., Sala, S., de la Peña, E., Gomis, A., & Viana, F. (2024). The ion channel TRPM8 is a direct target of the immunosuppressant rapamycin in primary sensory neurons. *British Journal of Pharmacology*, 1–23. <https://doi.org/10.1111/bph.16402>